Published by Institute of Physics Publishing for SISSA/ISAS

Received: *December 15, 2003*
Accepted: *February 11, 2004*

Realistic D-brane models on warped throats: fluxes, hierarchies and moduli stabilization

Juan F.G. Cascales, Maria Pilar García del Moral and Angel M. Uranga

Departamento de Física Teórica C-XI, and Instituto de Física Teórica C-XVI
Universidad Autónoma de Madrid
Cantoblanco, 28049 Madrid Spain
E-mail': juan.garcia@uam.es, gdelmoral@delta.ft.uam.es, angel.uranga@cern.ch

Fernando Quevedo

DAMTP, Centre for Mathematical Sciences, University of Cambridge
Cambridge CB3 0WA U.K.
E-mail: fernando.quevedo@cern.ch

Abstract: We describe the construction of string theory models with semirealistic spectrum in a sector of (anti) D3-branes located at an orbifold singularity at the bottom of a highly warped throat geometry, which is a generalisation of the Klebanov-Strassler deformed conifold. These models realise the Randall-Sundrum proposal to naturally generate the Planck/electroweak hierarchy in a concrete string theory embedding, and yielding interesting chiral open string spectra. We describe examples with standard model gauge group (or left-right symmetric extensions) and three families of SM fermions, with correct quantum numbers including hypercharge. The dilaton and complex structure moduli of the geometry are stabilised by the 3-form fluxes required to build the throat. We describe diverse issues concerning the stabilisation of geometric Kähler moduli, like blow-up modes of the orbifold singularities, via D term potentials and gauge theory non-perturbative effects, like gaugino condensation. This local geometry, once embedded in a full compactification, could give rise to models with all moduli stabilised, and with the potential to lead to de Sitter vacua. Issues of gauge unification, proton stability, supersymmetry breaking and Yukawa couplings are also discussed.

Keywords: Superstrings and Heterotic Strings, D-branes, Superstring Vacua.

JHEP02(2004)031

Contents

1. Introduction

Important progress has been made during the past few years regarding string theory model building. Chiral models resembling very much the structure of the standard model of particle physics have been explicitly constructed from type II and type I compactifications with D-branes (using e.g. D-branes at singularities and intersecting D-branes, see e.g. [1] for reviews). These models however leave open the question of moduli stabilisation. The few supersymmetric models explicitly constructed have not fully realistic spectra, and in addition have many moduli fields with flat potentials. The non-supersymmetric models lead to spectra closer to the standard model, but there is no good control of the scalar field potentials, and in most models they render the models unstable towards runaway zero-coupling or decompactification limits. A related further problem is that the smallness of electroweak scale, usually associated to a large size of the extra dimensions, is left unexplained in these models.

On the other hand, progress has been recently achieved in constructing non-realistic models with stabilisation of the dilaton and many geometric moduli via the introduction of a background of NSNS and RR field strength fluxes [2]–[4][1](in some cases, the remaining moduli may be stabilised via non-perturbatively generated superpotentials [7, 8]). Furthermore such flux compactifications naturally involve a string theory realisation of the Randall-Sundrum (RS) scenario [9], since they may lead to a hierarchy of scales by means of a warp factor in the higher dimensional metric, sourced by the energy carried by the flux background [10, 4].

A concrete construction reproducing the key features of the RS setup is provided by considering flux compactifications including a Klebanov-Strassler (KS) throat [11]. Namely, one considers compactification on Calabi-Yau spaces containing deformed conifold singularities [12], and introduces a large flux on the corresponding 3-sphere (and its dual cycle). The flux back-reaction on the metric creates a long throat, which ends smoothly at a tip containing the original 3-sphere supporting the flux. Since 3-form fluxes gravitate and carry 4-form charge, they create a supergravity background of the black 3-brane form, and the structure of the central region of the throat is an slice of anti-de Sitter space, AdS_5. The throat is cut off by the 3-sphere at the strongly warped end, and by the original Calabi-Yau compact space at the weakly warped end. These regions correspond to the infrared and ultraviolet branes in the RS construction [10, 4].

This is a very appealing scenario that includes several desirable properties, such as moduli fixing, natural hierarchy and de Sitter vacua. However there is no concrete proposal on how to include the standard model (or a gauge sector similar to it) in the scenario. This is the task we undertake in the present paper.

In order to generate the correct weak scale via the RS hierarchy, the standard model should be localised at the tip of the throat. A possibility would be to localise it on the world-volume of a set of D3-branes. However, moduli of D3-branes in imaginary self-dual fluxes of the kind discussed in [4] are not lifted. Hence one would have to face the problem of fixing these extra moduli, in order to explain the stabilisation of the D3-branes at the tip of the throat. An interesting alternative is to consider the SM to be localised on anti-D3-branes (denoted $\overline{\text{D3}}$-branes in what follows). These objects appear naturally in the construction of de Sitter vacua of string theory using flux stabilisation of moduli, in particular their tension is responsible for the lifting of the vacuum energy to a positive

[1]See [5, 6] for compactifications with fluxes and semirealistic spectra.

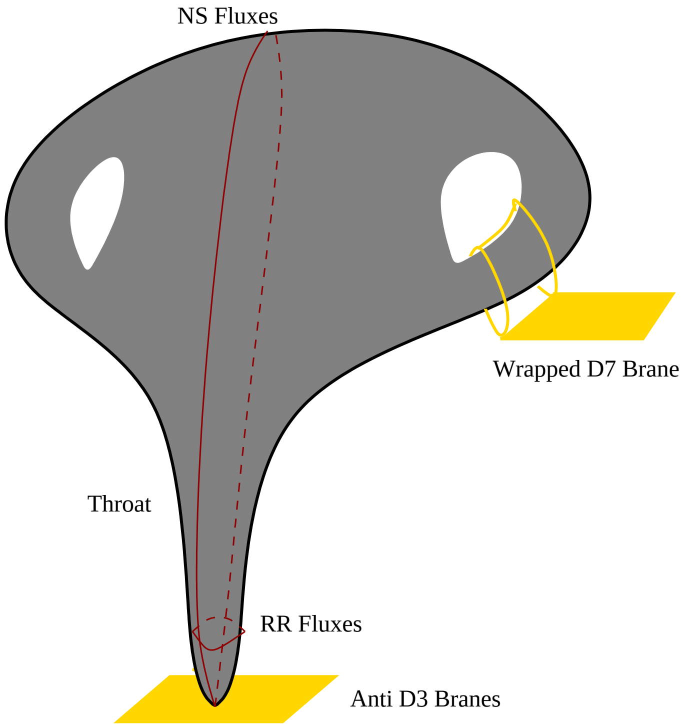

Figure 1: Description of a deformed conifold with 3-form fluxes (a KS throat) embedded in a compact geometry, with anti-D3-branes trapped at the tip of the throat. Beyond the throat, the compactifications may include other ingredients, like D7-branes wrapped on 4-cycles, etc, which are not relevant for the generation of the warp factor on the throat, but may lead to other interesting effects (like non-perturbative superpotentials).

value. In the setup including KS throats, anti-D3-branes are interesting because they are attracted by the fluxes and naturally fall to the tip of the throat [13]. Hence they are the natural objects to localise the standard model on their world-volume, and hence at the tip of the throat. A picture of the configuration is shown in figure 1. In the present paper we consider both possibilities.

Clearly, to obtain the standard model it is not enough to have a stack of D-branes, one needs the world-volume spectrum to lead to chiral fermions, with correct quantum numbers, etc. For D3-, $\overline{\rm D3}$-branes, the massless world-volume spectrum depends basically on the local geometry around them. It is then natural to apply previous results of D-brane model building to the present problem, in particular the bottom-up approach in [14] (see also [15]).

In [14] a new approach to build string models was proposed. The idea is to exploit the 'modular' structure for the string models constructed with D-branes (in other words, exploit locality in the extra dimensions). Namely, one first tailors a local D-brane configuration that can accommodate the standard model, and subsequently embeds it into different possible compactification manifolds. This approach separates the local properties of the models, such as the gauge group, the massless matter spectrum, running of gauge coupling, etc, from properties depending strongly on the global features of the compactification, such as supersymmetry breaking, scalar field potentials, etc.

A large class of local D-brane configurations leading to chiral 4d world-volume gauge sectors is provided by D3-branes (or $\overline{\rm D3}$-branes) at singularities. It is thus natural to combine techniques of model building with $\overline{\rm D3}$-branes at singularities with the construction of highly warped throats using deformed conifolds with fluxes. Indeed in this paper we construct explicit geometries containing deformed conifolds, and orbifold singularities sitting at the corresponding 3-spheres. Introduction of an explicit set of suitable 3-form fluxes leads to a warped throat, with the compact 3-cycles and the orbifold singularity at its tip. Finally introducing a set of $\overline{\rm D3}$-branes and D7-branes (all dynamically trapped at the tip of the throat) at the orbifold singularity, we obtain semirealistic chiral gauge sectors localised at the infrared end of the throat, so that their natural scale is strongly red-shifted with respect to the fundamental scale of the theory.

The paper is organised as follows. The next two sections are background material. In section 2 we briefly review the construction of chiral string models from D-branes at singularities. In section 3 we describe the introduction of fluxes in type IIB string theory compactifications, and their effect in fixing the dilaton and complex structure moduli, and in providing the string theory realisation of the Randall-Sundrum hierarchy via a strongly warped throat, based on a deformed conifold background (fluxes on a compact 3-sphere).

In section 4 we provide the explicit construction of a geometry containing a set of compact 3-spheres and $\mathbb{C}^3/\mathbb{Z}_3$ orbifold singularities. Sets of D-branes located at the latter naturally lead to chiral gauge sectors on their world-volume. We point out that the construction, involving a double elliptic fibration, naturally includes a $\mathbf{T^4}$ at the tip of the throat were D7 branes can wrap around. This allows to enrich the D-brane configurations at the tip of the throat, and improve the resulting chiral models. We also describe the introduction of a particular set of 3-form fluxes in this background, and the resulting stabilisation of complex structure moduli. These fluxes create a KS-like throat, with the D-brane configuration located at its tip.

In section 5 we present explicit examples of realistic models with the standard model gauge group or its left-right extensions. We present two classes of models depending on whether the standard model is realized on a stack of D3- or $\overline{\rm D3}$-branes. Section 6 is devoted to a discussion on how the extra moduli necessarily introduced by our construction can be fixed either by D-term potentials and/or nonperturbative effects. Finally, in section 7 we discuss some phenomenological properties of the models. We finish with some general discussions and open questions. Appendix A contains a technical point on the consistency of the set of fluxes we introduce in our geometry.

2. D-branes at singularities

Let us briefly review the bottom-up approach to phenomenological model building with D-branes at singularities. We centre our description on $\overline{\rm D3}$-branes at singularities. A more general and comprehensive discussion, centred on D3-branes, can be obtained from [14].

For concreteness we centre on $\mathbb{C}^3/\mathbb{Z}_N$ orbifold singularities, with $\mathbb{Z}_N$ generated by the action

$$(z_1, z_2, z_3) \to \left(\alpha^{l_1} z_1, \alpha^{l_2} z_2, \alpha^{l_3} z_3\right) \tag{2.1}$$

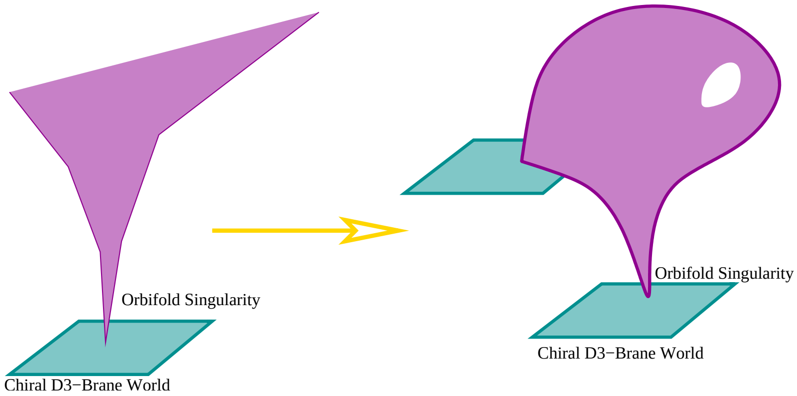

Figure 2: An illustration of the bottom-up approach. D3-branes at an orbifold singularity provide examples of chiral theories in which the standard model can be embedded. Most of the properties of the model depend on the structure of the singularity. This local model can then be embedded in many different string compactifications, as long as the compact manifold has the same type of orbifold singularity.

with $\alpha = e^{2\pi i/N}$. For $l_1+l_2+l_3 = 0$ mod N the orbifold preserves an $\mathcal{N}=2$ supersymmetry in the bulk, further reduced to $\mathcal{N}=1,0$ when D-branes are introduced. We restrict to this situation, since non-supersymmetric orbifolds contain closed string tachyons in twisted sectors, which complicate the system.

Let us introduce a set of n $\overline{\mathrm{D3}}$-branes spanning $\mathbf{M_4}$ and sitting at the singular point in $\mathbb{C}^3/\mathbb{Z}_N$. Before the orbifold projection, the set of $\overline{\mathrm{D3}}$-branes in flat space leads to a $\mathcal{N}=4$ $U(n)$ world-volume gauge theory. Decomposing it with respect to the $\mathcal{N}=1$ supersymmetry preserved by the branes, we have a $U(n)$ vector multiplet V, and three chiral multiplets Φ_a in the adjoint representation. The world-volume gauge field theory for $\overline{\mathrm{D3}}$-branes at the orbifold geometry is obtained [16] from the above one by keeping the $\mathbb{Z}_N$-invariant states. The $\mathbb{Z}_N$ has a geometric action on Φ_a, similar to (2.1), and an action on the gauge degrees of freedom, given by conjugation of the Chan-Paton wavefuncion λ by an $n\times n$ unitary matrix $\gamma_{\theta,\bar{3}}$ or order N.

$$\lambda \to \gamma_{\theta,\bar{3}}\,\lambda\,\gamma_{\theta,\bar{3}}^{-1}\,. \tag{2.2}$$

Without loss of generality, $\gamma_{\theta,\bar{3}}$ can be diagonalised, to take the simple form

$$\gamma_{\theta,\bar{3}} = \mathrm{diag}\left(\mathbb{1}_{n_0}, \alpha\mathbb{1}_{n_1}, \ldots, \alpha^{N-1}\mathbb{1}_{n_{N-1}}\right). \tag{2.3}$$

Here $\mathbb{1}_{n_k}$ is the identity matrix in n_k dimensions, and integers n_k satisfy $\sum_k n_k = n$.

Imposing invariance under the combined geometric and Chan-Paton $\mathbb{Z}_N$ actions, we have the projections

$$V\ :\ \lambda = \gamma_{\theta,\bar{3}}\,\lambda\,\gamma_{\theta,\bar{3}}^{-1}\,; \qquad \Phi_a\ :\ \lambda = \alpha^{l_a}\,\gamma_{\theta,\bar{3}}\,\lambda\,\gamma_{\theta,\bar{3}}^{-1}\,. \tag{2.4}$$

The resulting spectrum of $\mathcal{N}=1$ multiplets is

$$\mathcal{N}=1 \text{ Vect.Mult.} \qquad U(n_0)\times U(n_1)\times\cdots\times U(n_{N-1})$$

$$\mathcal{N}=1 \text{ Ch.Mult} \qquad \sum_{a=1}^{3}\sum_{i=0}^{N-1}(\mathbf{n}_i,\overline{\mathbf{n}}_{i+l_a}) \tag{2.5}$$

with the index i defined modulo N. This kind of spectrum is usually encoded in quiver diagrams, where gauge factors are represented by nodes, and bi-fundamental fields $(n_i,\overline{n}_j)$ are represented by oriented arrows from the i^{th} to the j^{th} node, see below.

From (2.5) we can extract a very simple but powerful conclusion: Only for the $\mathbb{Z}_3$ orbifold, $(l_1,l_2,l_3)=(1,1,-2)$, will we get a matter spectrum arranged in three identical copies or families. Indeed, only for that case we have $l_1=l_2=l_3$ mod N. Therefore, and quite remarkably, the maximum number of families for this class of models is three, and it is obtained for a unique twist, the $\mathbb{Z}_3$ twist.

It is important to realise that a consistent configurations of D-branes should obey cancellation of tadpoles for RR fields with compact support in the transverse space. This in particular guarantees cancellation of non-abelian anomalies, and the cancellation of mixed $U(1)$ anomalies via a Green-Schwarz mechanism [17]. If only $\overline{\text{D3}}$-branes are present at the orbifold singularity, the RR tadpole cancellation condition reads

$$\prod_{a=1}^{3} 2\,\sin\left(\frac{\pi k l_a}{N}\right)\,\mathrm{Tr}\gamma_{\theta^k,\bar{3}}=0\,. \tag{2.6}$$

For $\mathbb{Z}_3$ this implies $n_0=n_1=n_2$, which only allows for phenomenologically unattractive possibilities (and does not allow for more promising ones e.g. $n_0=3, n_1=2, n_2=1$).

This can be improved by enriching the configurations, introducing other kinds of D-branes passing through the singularity. We will centre on D7-branes spanning two complex planes in the six extra dimensions, which are a natural ingredient in IIB flux compactifications [4]. For concreteness, we centre on a stack of w D7$_3$-branes, spanning the submanifold $z_3=0$ in the geometry, hence transverse to the third complex plane, which we assume has even l_3.

Hence, in addition to the $\bar{3}\bar{3}$ spectrum, there is a sector of $\bar{3}7+7\bar{3}$ open strings.[2] Before the orbifold projection, it leads to a 4d $\mathcal{N}=2$ hypermultiplet transforming in the bi-fundamental representation $(n,\bar{w})$. In order to quotient by the orbifold action, one should introduce an $w\times w$ Chan-Paton matrix $\gamma_{\theta,7_3}$ implementing it in the D7-brane gauge degrees of freedom

$$\gamma_{\theta,7_3}=\mathrm{diag}\left(\mathbb{1}_{w_0},\alpha\mathbb{1}_{w_1},\ldots,\alpha^{N-1}\mathbb{1}_{w_{N-1}}\right). \tag{2.7}$$

In addition we have the geometric action of $\mathbb{Z}_N$ on the $\bar{3}7+7\bar{3}$ fields. Since the orbifold breaks the supersymmetry preserved by the D7- and the $\overline{\text{D3}}$-branes, scalars and fermions pick up different geometric phases. The projection conditions read

$$\text{Cmplx.Scalar}: \lambda_{\bar{3}7}=\gamma_{\theta,\bar{3}}\lambda_{\bar{3}7}\gamma^{-1}_{\theta,7_3}\,;\quad \text{4d Weyl Ferm.}: \lambda_{\bar{3}7}=e^{-i\pi l_3/N}\gamma_{\theta,\bar{3}}\lambda_{\bar{3}7}\gamma^{-1}_{\theta,7_3} \tag{2.8}$$

[2]The 77 open string sector is more dependent on global features of the compactification. We skip it for the moment, but include it explicitly in our examples.

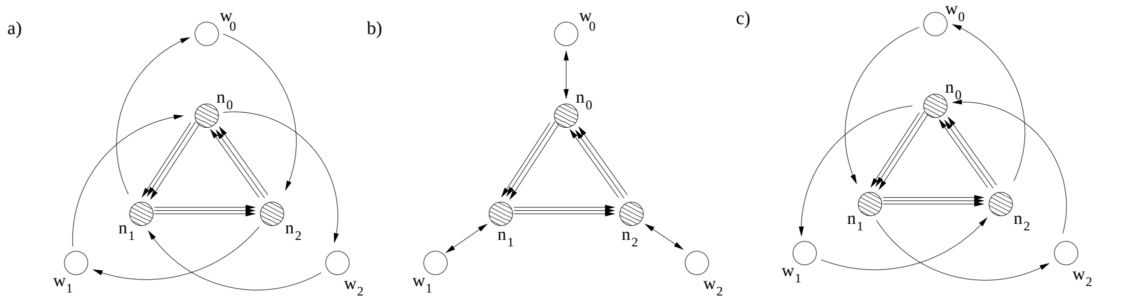

Figure 3: This is the quiver diagram corresponding to a general $\mathbb{C}^3/\mathbb{Z}_3$ model. In the non-SUSY case (models with $\overline{\text{D3}}$ and D7-branes), fermions and scalars transform in different representations of the gauge group, namely those displayed (respectively) in (a) and (b). For the supersymmetric case, both scalars and fermions fill in chiral multiplets of the preserved SUSY, and transform in the bifundamentals displayed in (c).

The resulting spectrum is

$$\begin{array}{ll} \text{Cmplx.Scalars} & \sum_{i=0}^{N-1} \left[\, (\mathbf{n}_i, \bar{\mathbf{w}}_i) + (\bar{\mathbf{n}}_i, \mathbf{w_i})\, \right] \\ \text{4d Weyl Ferm.} & \sum_{i=0}^{N-1} \left[\left(\bar{\mathbf{n}}_i, \mathbf{w_{i-\frac{1}{2}l_3}}\right) + \left(\mathbf{n}_{i-\frac{1}{2}l_3}, \bar{\mathbf{w}}_i\right) \right]. \end{array} \tag{2.9}$$

The RR tadpole cancellation condition reads

$$\prod_{a=1}^{3} 2\sin\left(\frac{\pi k l_a}{N}\right) \mathrm{Tr}\gamma_{\theta^k,\bar{3}} - 2\sin\left(\frac{\pi k l_3}{N}\right) \mathrm{Tr}\gamma_{\theta^k,7_3} = 0\,. \tag{2.10}$$

For the interesting case of $\mathbb{Z}_3$, the full $\bar{3}\bar{3}$ and $\bar{3}7 + 7\bar{3}$ spectrum on the $\overline{\text{D3}}$-brane world-volume is

$$\begin{array}{lll} \bar{3}\bar{3} & \mathcal{N}=1 \text{ Vect.Mult.} & U(n_0)\times U(n_1)\times U(n_2) \\ & \mathcal{N}=1 \text{ Ch.Mult} & 3\,[\,(n_0,\bar{n}_1) + (n_1,\bar{n}_2) + (n_2,\bar{n}_0)\,] \\ \bar{3}7+7\bar{3} & \text{Cmplx.Scalars} & [(n_0,\bar{w}_0)+(n_1,\bar{w}_1)+(n_2,\bar{w}_2)+(\bar{n}_0,w_0)+(\bar{n}_1,w_1)+(\bar{n}_2,w_2)] \\ & \text{4d Weyl Ferm.} & [(n_0,\bar{w}_2)+(n_1,\bar{w}_0)+(n_2,\bar{w}_1)+(\bar{n}_2,w_0)+(\bar{n}_0,w_1)+(\bar{n}_1,w_2)]\,. \end{array} \tag{2.11}$$

Let us finally provide the spectrum for a system of D3- and D7-branes. Following [14] we can consider for a configuration of D3-branes (with CP matrix $\gamma_{\theta,3}$ given by (2.3) and D7-branes, as above. The resulting $\mathcal{N}=1$ supersymmetric spectrum is

$$\begin{array}{lll} 33 & \mathcal{N}=1 \text{ Vect.Mult.} & U(n_0)\times U(n_1)\times U(n_2) \\ & \mathcal{N}=1 \text{ Ch.Mult} & 3\,[\,(n_0,\bar{n}_1) + (n_1,\bar{n}_2) + (n_2,\bar{n}_0)\,] \\ 37+73 & \mathcal{N}=1 \text{ Ch.Mult} & [(n_0,\bar{w}_1)+(n_1,\bar{w}_2)+(n_2,\bar{w}_0)+(\bar{n}_0,w_2)+(\bar{n}_1,w_0)+(\bar{n}_2,w_1)]\,. \end{array} \tag{2.12}$$

This general spectrum is encoded in the quiver diagram shown in figure 3. The RR tadpole conditions read

$$\pm 3\mathrm{Tr}\gamma_{\theta,3} - \mathrm{Tr}\gamma_{\theta,7_3} = 0 \tag{2.13}$$

with the upper (lower) sign corresponding to the $\overline{\text{D3}}$- (resp, D3-) brane case.

3. Flux compactifications and the Klebanov-Strassler throat

There is much recent interest in the study of compactifications of type IIB on Calabi-Yau (CY) threefolds (or generalisations in terms of F-theory on CY fourfolds) with non-trivial backgrounds for NSNS and RR 3-form field strength fluxes, H_3 and F_3 respectively [2]–[4].

These compactifications have several interesting features. One of them is that they naturally have very few moduli. Namely, the fluxes induce a potential for the scalar moduli of the underlying Calabi-Yau compactification, lifting the corresponding flat directions and stabilising most of them, in particular the dilaton and all complex structure moduli. The stabilisation can be intuitively understood as follows. The equations of motion require the flux combination $G_3 = F_3 - iSH_3$ (where $S = 1/g_s - ia$ is the complex IIB dilaton) to be imaginary self-dual with respect to the underlying CY metric, $G_3 = i *_{6d} G_3$. Since the fluxes F_3, H_3 are quantised, the flux density G_3 depends on complex structure moduli (which control the size of 3-cycles), in addition to the dilaton. Hence, for the imaginary self-duality condition to hold, the dilaton and complex structure moduli must take particular vacuum expectation values, hence they are stabilised by the the choice of flux quanta.

In 4d effective supergravity terms, the fluxes generate a superpotential [3]:

$$W \;=\; \int_M G_3 \wedge \Omega \,, \tag{3.1}$$

where Ω is the holomorphic 3-form in the Calabi-Yau space. This depends implicitly on the dilaton and complex structure moduli. Minimisation of the scalar potential leads to the imaginary self-duality condition, and to the moduli stabilisation described above.

Since the superpotential does not depend on Kähler moduli, they do not appear in the scalar potential, and they are not stabilised by the flux background. For instance, centring on the overall Kähler size of the Calabi-Yau T, the Kähler potential is

$$K = \tilde{K}(\varphi_i, \varphi_i^*) - 3\log\left(T + T^*\right), \tag{3.2}$$

with $\tilde{K}$ the Kähler potential for all the other fields φ_i except for T. The supersymmetric scalar potential takes the form

$$V_{SUSY} \;=\; e^K \left(K^{i\bar{j}} D_i W \overline{D_j W} \right), \tag{3.3}$$

with $K^{i\bar{j}}$ the inverse of the Kähler metric $K_{i\bar{j}} = \partial_i \partial_{\bar{j}} K$ and $D_i W = \partial_i W + W \partial_i K$ the Kähler covariant derivative. The contribution of T to the scalar potential through the Kähler potential precisely cancels the term $-3e^K|W|^2$ of the standard supergravity potential, as usual in no-scale models [18]. The potential is positive definite, so the minimum lies at $V = 0$, with all the fields except for T fixed from the conditions $D_i W = 0$. This minimum is supersymmetric if $D_T W = W = 0$ and not supersymmetric otherwise.

Additional ingredients have been proposed to stabilise the additional Kähler moduli. For the case of a single modulus, it was argued in [7] that non-perturbative effects on a D7-brane gauge sector can stabilise it, leading to anti-de Sitter vacua. Further addition of anti-D3-branes could then be employed to turn the vacuum into a de Sitter vacuum.

JHEP02(2004)031

A second important property of these compactifications is that they naturally lead to warped metrics. Namely, the internal background metric is not the Ricci-flat one for the Calabi-Yau, but conformal to it, due to a non-trivial warp factor,

$$ds^2 \;=\; Z^{-1/2}\,\eta_{\mu\nu}\,dx^\mu\,dx^\nu \;+ Z^{1/2}ds^2{}_{CY}\,. \tag{3.4}$$

The warp factor is due to the flux backreaction on the metric

$$\nabla^2 Z \;\simeq\; G^*_{lmn}\,G^{lmn} \tag{3.5}$$

(where ∇ and the raising of indices are done with the underlying CY metric $ds^2{}_{CY}$). The warp factor implies that the 4d scales of physical processes suffer a redshift which depends on the point of the internal space at which they take place. This effect can be quite strong in highly warped configurations, and provides the string theory realisation of the Randall-Sundrum hierarchy. In this reference, exponential warp factors were proposed in [9] as a way to solve the hierarchy between the weak and the Planck scale. The particular setup employs a 5d geometry, given by a slice of AdS_5 space between two $\mathbf{M_4}$ boundaries, denoted infrared/ultraviolet regions according to their large/small redshift factor, respectively. The standard model fields were assumed to be localised at the infrared region, so that any Planck scale effect is lowered to the TeV scale due to the warp factor, explaining the hierarchy between the electroweak and 4d Planck scales.

There is a simple geometry with fluxes, which illustrates both these aspects of flux compactifications. It is the Klebanov-Strassler (KS) throat [11]. The underlying Calabi-Yau is the deformed conifold, a non-compact manifold described as the complex hypersurface

$$x_1^2 \,+\, x_2^2 \,+\, x_3^2 \,+\, x_4^2 \;=\; \epsilon \tag{3.6}$$

in $\mathbb{C}^4$. There is a complex structure modulus, whose vev is ϵ. It controls the size of the unique compact non-trivial 3-cycle in the geometry, which is the $\mathbf{S^3}$ obtained (e.g. for ϵ real) by taking real x_i in (3.6). Its dual 3-cycle is non-compact, and it is convenient to introduce a cutoff Λ to render its volume finite.[3] Introducing M units of flux F_3 over this $\mathbf{S^3}$, and $-K$ units of H_3 flux over the dual cycle, leads to stabilisation of the complex structure modulus at the value

$$\epsilon = \exp\left(-\frac{2\pi K}{M g_s}\right). \tag{3.7}$$

The full metric is described in [11]. The geometry has the structure of a highly warped throat, looking like AdS_5 space (times an internal compact geometry $T^{1,1} = \mathbf{S^2}\times\mathbf{S^3}$) in its central region. However, the finite size of the $\mathbf{S^3}$ caps off the throat at a finite distance, leading to a maximum warp factor at the bottom of the throat given by

$$Z \sim e^{8\pi K/3Mg_s} \tag{3.8}$$

In compactifications, the other end of the throat (the mouth) ends in the (slightly warped, almost flat) geometry of the Calabi-Yau. The situation is shown in figure 1.

[3] If the conifold is embedded in a global compactification, the volume of this cycle is indeed finite.

JHEP02(2004)031

As emphasised in [10, 4], the situation is highly reminiscent of [9], with a region looking like an slice of AdS_5 space, ending at the infrared (by the finite size $\mathbf{S^3}$) and at the ultraviolet (by the remaining piece of the compact Calabi-Yau). In fact, this was advocated in [4], as a string theory realisation of the Randall-Sundrum proposal. However, a concrete realisation where there is a realistic gauge sector localised at the bottom of the throat has not been achieved in the literature. Our purpose in the present paper is to provide explicit examples of this kind.

4. Orbifolds within conifolds

4.1 More on the conifold

We are interested in constructing a strongly warped throat, similar to the KS model, at the bottom of which we have an orbifold singularity (preferably $\mathbb{C}^3/\mathbb{Z}_3$), on which we would like to place anti-D3-branes to lead to a chiral gauge sector. This can be achieved by starting with a Calabi-Yau geometry including a set of 3-cycles (preferably 3-spheres) and a $\mathbb{C}^3/\mathbb{Z}_3$ singularity lying on them. Introduction of large fluxes on those 3-cycles (and their duals) would generate a highly warped throat, at the tip of which the singularity sits.

A simple possibility would be to construct the quotient of the deformed conifold by a $\mathbb{Z}_3$ action with isolated fixed points. Unfortunately, the deformed conifold does not admit such symmetries. For instance, we can change variables and write (3.6) as

$$xy - uv = \epsilon\,. \tag{4.1}$$

There is a $\mathbb{Z}_3$ symmetry $(x,u) \to e^{2\pi i/3}(x,u)$ and $(y,v) \to e^{-2\pi i/3}(y,v)$, which unfortunately is freely acting. Other possible $\mathbb{Z}_3$ symmetries, like $x \to e^{2\pi i/3}x$, $y \to e^{-2\pi i/3}y$, leaving u, v invariant, have a whole complex curve (defined by $uv = \epsilon$) of fixed points, so that locally the singularity is $\mathbb{C} \times \mathbb{C}^2/\mathbb{Z}_3$. This singularity leads to $\mathcal{N} = 2$ world-volume theories on $\overline{\mathrm{D3}}$-brane probes, which are non-chiral and thus not interesting.

Hence, it is not possible to consider a deformed conifold invariant under a $\mathbb{Z}_3$ symmetry of the required kind. An alternative is to construct geometries including several deformed conifolds, arranged in an invariant way under a suitable $\mathbb{Z}_3$ symmetry, by which we subsequently quotient the geometry. This is accomplished in next subsections, but before we need some additional information on the conifold.

The deformed conifold (4.1) can be equivalently described by

$$xy = z - \frac{\epsilon}{2}\,; \qquad uv = z + \frac{\epsilon}{2}\,. \tag{4.2}$$

In this description, the coordinate z parametrises a complex plane, at each point of which the coordinates x, y (subject to the equation) describe a $\mathbb{C}^*$ fibration (with a fiber topologically $\mathbb{R} \times \mathbf{S^1}$). The fiber degenerates to two complex planes at the point $z = \epsilon/2$, where we have $xy = 0$. Finally there is an analogous $\mathbb{C}^*$ fibration parametrised by u, v, and degenerating at $z = -\epsilon/2$. See figure 4.

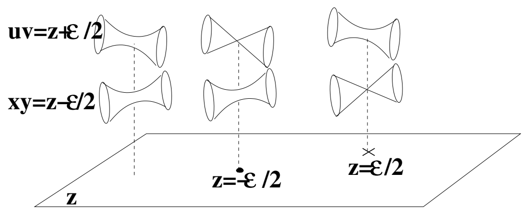

Figure 4: Description of the conifold geometry as a double $\mathbb{C}^*$ fibration.

The $\mathbf{S^3}$ in the deformed conifold is visible as follows. In each of the two $\mathbb{C}^*$ fibers there is an $\mathbf{S^1}$, which shrinks to zero size at $z = \pm\epsilon/2$, respectively. Consider the 3-cycle obtained by taking a real segment in the z-plane joining the points $z = \epsilon/2$ and $z = -\epsilon/2$, and fibering over it the $\mathbf{S^1}$ fiber in the first $\mathbb{C}^*$ fibration and the $\mathbf{S^1}$ fiber in the second $\mathbb{C}^*$ fibration. This defines a 3-cycles without boundary, which topologically is $\mathbf{S^3}$, and whose size is controlled by the parameter ϵ. Our pictorial depiction of those cycles is shown in figure 5.

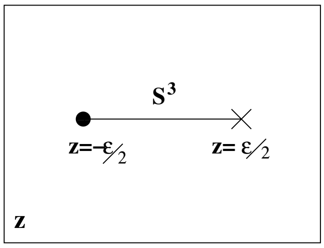

Figure 5: Simplified pictorial depiction of the conifold and its $\mathbf{S^3}$. The dot and the cross denote the degeneration points of the two $\mathbb{C}^*$ fibrations, respectively.

4.2 Elliptic fibrations and Schoen's Calabi-Yau

In this section we describe geometries containing several deformed conifolds.

Let us start by considering the two-fold defined by

$$y^2 = x^3 + f(z)x + g(z)\,, \tag{4.3}$$

where f, g are holomorphic polynomials (whose degree is constrained, although we momentarily skip this point). It describes an elliptic fibration over a complex plane, in Weierstrass form. Namely z parametrises a complex plane, and at each point in z the variables x, y parametrise a two-torus (i.e. elliptic curve). The fiber is degenerate on top of the points z satisfying the discriminant equation

$$\Delta = 4f(z)^3 + 27g(z)^2 = 0 \tag{4.4}$$

at which a (p, q) 1-cycle of the two-torus pinches to zero size. Near each of these degenerations, say at $z = z_0$, one can introduce local complex coordinates in the torus u, v, such that the geometry is locally $uv = z - z_0$. Namely the local geometry corresponds to a $\mathbb{C}^*$ fibration near a degeneration point, see figure 6.

Hence, geometries with deformed conifold singularities can be constructed by considering double elliptic fibrations. Namely, consider the threefold

$$y^2 = x^3 + f(z)x + g(z)\,; \qquad y'^2 = x'^3 + f'(z)x' + g'(z) \tag{4.5}$$

describing two elliptic fibrations over the z-plane. The above equation can be used to define a compact Calabi-Yau manifold, by considering z to parametrise (a patch) in $\mathbb{P}_1$ (i.e. by

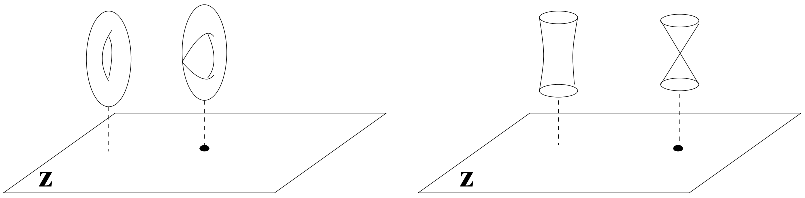

Figure 6: The degeneration of an elliptic fibration near a degenerate fiber can be locally described as a $\mathbb{C}^*$ fibration.

homogenising (4.5) with respect to projective coordinates $[z, w]$ for $\mathbb{P}_1$), and imposing the polynomials f, f' and g, g' to be homogeneous of degree 4 and 6, respectively. Such compact geometries have been studied in [19]. In general, we will be interested in local models, namely non-compact versions of (4.5), so we regard z as parameterising a complex plane, and take f, f', g, g' of low enough degree. Schoen's manifold then provides a possible global embedding of these local models in a compact Calabi-Yau.

Using the above information, one can see that such geometries contain non-trivial compact 3-cycles. Denote z_i, z'_j the degeneration points of each fibration, and (p_i, q_i), (p'_j, q'_j) the 1-cycles in the corresponding elliptic fiber degenerating at those points. An $\mathbf{S^3}$ is obtained by considering a segment in the z-plane joining a point z_i with a point z'_j, and fibering over it the (p_i, q_i) 1-cycle of the first elliptic fibration times the (p'_j, q'_j) 1-cycle of the second. For geometries with coinciding z_i and z'_j, the $\mathbf{S^3}$ has zero size and we get a conifold singularity. If they are close but not coincident, then locally we have a deformed conifold, with deformation parameter $\epsilon_{ij} = z_i - z'_j$.

4.3 The $\mathbb{Z}_3$-invariant manifold

We would like to consider geometries invariant under a $\mathbb{Z}_3$ action with isolated fixed points. A suitable $\mathbb{Z}_3$ symmetry is provided by $z \to e^{2\pi i/3}z$, $x \to e^{2\pi i/3}x$, $x' \to e^{2\pi i/3}x'$ Manifolds with this $\mathbb{Z}_3$ symmetry are of the form

$$\begin{aligned} y^2 &= x^3 + f_2 z^2 x + (g_2 z^6 + g_1 z^3 + g_0) \\ y'^2 &= x'^3 + f'_2 z^2 x' + (g'_2 z^6 + g'_1 z^3 + g'_0)\,. \end{aligned} \tag{4.6}$$

Fixed points lie on top of $z = 0$, where the elliptic fibers are $\mathbb{Z}_3$ symmetric $\mathbf{T^2}$'s, namely their complex structure parameter corresponds to $\tau = e^{2\pi i/3}$. The $\mathbb{Z}_3$ action has three fixed points on each, so in total the geometry has nine isolated fixed points, around which the geometry is locally $\mathbb{C}^3/\mathbb{Z}_3$.

We are interested in constructing a simple as possible geometry. Hence we can impose the elliptic fibrations to have just three degeneration points, so that the geometry, roughly speaking, contains three copies of the deformed conifold, rotated to each other by the $\mathbb{Z}_3$. Without loss of generality, such geometries read

$$\begin{aligned} y^2 &= x^3 - 3\left(\frac{z}{z_0}\right)^2 x + 2\left(\frac{z}{z_0}\right)^3 - 4 \\ y'^2 &= x'^3 - 3\left(\frac{z}{z'_0}\right)^2 x' + 2\left(\frac{z}{z'_0}\right)^3 - 4\,. \end{aligned} \tag{4.7}$$

This describes an elliptic fibration degenerating at points $z = \omega z_0$, and another elliptic fibration degenerating at $z = \omega z'_0$, where $\omega = 1$, $e^{2\pi i/3}$, $e^{-2\pi i/3}$. Clearly z_0 or z'_0 can be eliminated by a rescaling of z, but we prefer to keep the above more symmetric description of the manifold. In the above geometry, the 1-cycles degenerating at the different point, may be chosen to be the cycles $(2, -1)$, $(-1, 2)$ and $(-1, -1)$, and analogously for the primed fibration. This double elliptic fibration was considered (in a different context) in [20, section 3.2].

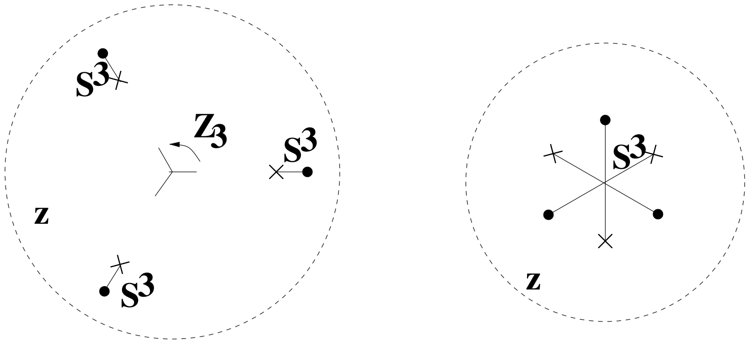

Figure 7: The first figure shows the a general $\mathbb{Z}_3$-invariant configuration for the three deformed conifolds. In the second figure we show a configuration invariant under an additional $\mathbb{Z}_2$ symmetry.

A pictorial depiction of geometries of this kind are shown in figure 7. The first figure is the general kind of configuration. The second shows the geometry at a point in moduli space where it has an additional $\mathbb{Z}_2$ symmetry, given by $x, y \to x', y'$, $z \to -z$, that we will exploit below. Our final geometry is obtained by modding out the manifold (4.7) by the $\mathbb{Z}_3$ symmetry, which has nine fixed points.

4.4 Introduction of D-branes

One can now introduce D-branes in this local geometry, to obtain chiral gauge sectors. In particular, we will introduce D3- or $\overline{\mathrm{D3}}$-branes sitting at the $\mathbb{C}^3/\mathbb{Z}_3$ orbifold points, and D7-branes located at $z = 0$, hence passing through the singularities, and wrapped on the $\mathbf{T^4}$ fiber in the geometry. These sets of D-branes lead to a chiral open string spectrum localised on their world-volume. The models are such that the standard model group and matter multiplets are located on D3- or $\overline{\mathrm{D3}}$-branes at the origin in the z-plane and elliptic fibers.

The simplest option, which already provides a chiral gauge sector, is to locate a number n of $\overline{\mathrm{D3}}$-branes at the orbifold point at the origin. It leads to a $U(n)^3$ world-volume gauge theory with $\mathcal{N} = 1$ supersymmetry (ignoring the effect of the fluxes) and chiral matter multiplets in the three copies of the representation $(n, \bar{n}, 1) + (1, n, \bar{n}) + (\bar{n}, 1, n)$.

Although chiral, this theory is not realistic. More interesting models can be obtained exploiting a further natural ingredient in flux compactifications, namely by introducing D7-branes, passing through the origin. Their presence allows to consider richer Chan-Paton structures for the $\overline{\mathrm{D3}}$-branes, consistently with twisted RR tadpole cancellation, and to build models with gauge group and matter closer to the standard model. Explicit D-brane configurations of this kind are discussed in section 5.

In the next subsection we describe the introduction of fluxes in this geometry, in order to create a highly warped KS-like throat, and consider a choice of fluxes which ensures (via moduli stabilisation) that the singularities (and hence the D-brane configuration and the gauge sector) sit at the bottom of the highly warped throat.

An important question is the backreaction of the branes on the underlying geometry. This can be considered small as long as the flux quanta are larger than the number of D-

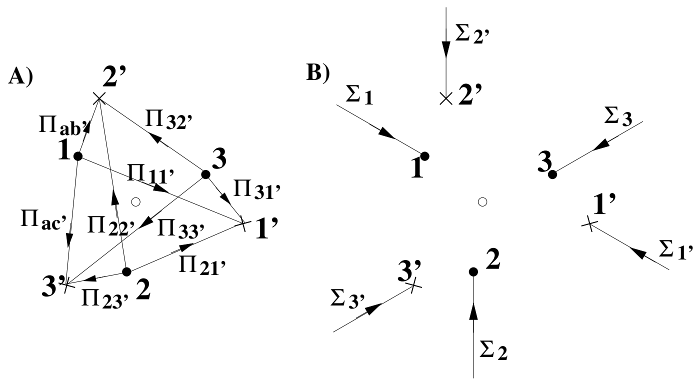

Figure 8: Pictorial depiction of some interesting 3-cycles in our geometry. Figure 7a shows the compact 3-cycles, in three different orbits of the $\mathbb{Z}_3$ action. Figure 7b shows the non-compact 3-cycles, which lie in two $\mathbb{Z}_3$ orbits.

branes required, a situation which can be achieved consistently with the desired hierarchy (e.g. by rescaling the fluxes keeping the hierarchy (3.8) constant). A second important point is that the chiral part of the D-brane world-volume spectrum can be read off from the configuration without fluxes, since is protected by chirality. Non-chiral fields massless in the absence of fluxes, may however receive flux-induced mass terms.

4.5 Turning on fluxes and the structure of the throat

We would now like to turn on 3-form fluxes on the 3-cycles in our geometry, and build a highly warped KS-like throat. We choose to introduce RR fluxes on the compact 3-cycles and NSNS fluxes on non-compact 3-cycles in the geometry. The flux we introduce stabilises the complex structure modulus (that can be considered to be z_0/z_0'), and leads to a geometry with small $\mathbf{S^3}$s, lying at the bottom of the throat.

Moreover, we would like the final geometry to contain the $\mathbb{C}^3/\mathbb{Z}_3$ orbifold singularity at the bottom of the throat. This is ensured if the final value of z_0/z_0' is such than the origin is on some $\mathbf{S^3}$ with non-zero flux. Figure 7a shows a situation where this would not be the case, namely where the throat develops and the $\mathbb{C}^3/\mathbb{Z}_3$ singularity is left behind, in the almost unwarped part of the Calabi-Yau. On the other hand, figure 7b shows a situation where there are 3-spheres passing through the origin. This implies that, when we introduce fluxes on them and the throat develops, the origin will lie at the bottom of the throat.

In general, and for such a complicated geometry, it is difficult to determine the value at which moduli stabilise, in terms of the flux quanta. In this paper we do not solve this problem systematically, but rather notice that the interesting case in figure 7b is invariant under the $\mathbb{Z}_2$ symmetry discussed at the end of section 4.3. It is then expected that a $\mathbb{Z}_2$-invariant set of flux quanta assignments will ensure the moduli stabilise at precisely such geometry.

Since we are not interested in the most general flux, we do not require a full knowledge of a basis of 3-cycles in the geometry. The only requirement in introducing the fluxes is the consistency condition that homologically related 3-cycles get similarly related fluxes.

In our geometry there are three kinds of $\mathbf{S^3}$'s shown in figure 8a, corresponding to three $\mathbb{Z}_3$ orbits. We denote by $\Pi_{ij'}$ $(i,j = 1,2,3)$ the 3-cycle defined by the segment joining the degenerations with labels i and j'. The three classes are $\Pi_{11'}$ (and its images $\Pi_{22'}$, $\Pi_{33'}$), $\Pi_{12'}$ (and images $\Pi_{23'}$, $\Pi_{31'}$) and $\Pi_{13'}$ (and images $\Pi_{21'}$, $\Pi_{32'}$). There are also some non-compact 3-cycles, shown in figure 8b, which lie in two $\mathbb{Z}_3$ orbits. They are denoted Σ_i and $\Sigma_{i'}$.[4]

The $\mathbb{Z}_3$ acts as a simultaneous cyclic rotation of $(1,2,3)$ and $(1',2',3')$, and leaves the geometry invariant. The $\mathbb{Z}_2$ action is $[\Pi_{ij'}] \to [\Pi_{ji'}]$, $[\Sigma_i] \leftrightarrow [\Sigma_{i'}]$, and is a symmetry of the homology lattice, but in general not a symmetry of the geometry. For $z_0 = -z_0'$, the $\mathbb{Z}_2$ is a symmetry of the geometry as well.

As suggested above, there are several homology constraints among the above set of 3-cycles, which our flux assignments should respect. Some of the relevant ones for us are described in appendix A, in terms of deformation arguments. The basic relation reads

$$3[\Sigma_3] - 3[\Sigma_2] = [\Pi_{11'}] + [\Pi_{12'}] + [\Pi_{13'}] \tag{4.8}$$

and similar ones among their $\mathbb{Z}_3$ images. This implies that if the flux over $[\Sigma_2]$ and $[\Sigma_3]$ are equal (as required by $\mathbb{Z}_3$ symmetry), then the sum of fluxes over $[\Pi_{11'}]$, $[\Pi_{12'}]$, $[\Pi_{13'}]$, must vanish. If we are interested in a $\mathbb{Z}_2$ invariant assignment of fluxes, then (using also the $\mathbb{Z}_3$ symmetry) the flux over $[\Pi_{12'}]$ and $[\Pi_{13'}]$ must be equal, and then the flux over $[\Pi_{11'}]$ must be (minus) twice that amount. Similar statements follow for the $\mathbb{Z}_3$-related images of these cycles.

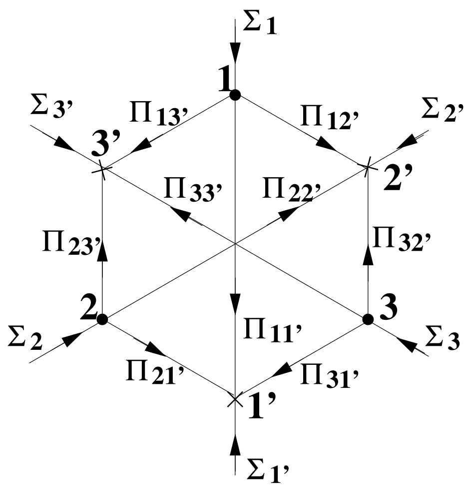

Figure 9: The figures shows the set of 3-cycles on which we have turned on a $\mathbb{Z}_2$-invariant set of 3-form fluxes. The moduli stabilise at the shown $\mathbb{Z}_2$-invariant geometry.

The final configuration of fluxes is therefore

$$\int_{[\Pi_{ii'}]} F_3 = K\,, \qquad \int_{[\Pi_{ij'}]} F_3 = -\frac{K}{2} \qquad \text{for } i \neq j$$
$$\int_{[\Sigma_i]} H_3 = -\int_{[\Sigma_{i'}]} H_3 = M \tag{4.9}$$

and succeeds in providing a set of $\mathbb{Z}_2$-invariant fluxes. Hence they stabilise the moduli at the $\mathbb{Z}_2$-invariant geometry, namely $z_0 = -z_0'$. In such situation, the orbifold points in the $\mathbb{Z}_3$ quotient lie on the 3-sphere associated to the orbit $\Pi_{ii'}$, so that the orbifold point is at the bottom of the throat. The final picture for the 3-cycles with flux, and the resulting geometry, is in figure 9.

It is also important to notice that the different $\mathbf{S^3}$ (related by $\mathbb{Z}_3$) in the covering space wrap in different directions in the $\mathbf{T^4}$, and that their size is thus related to the local size of $\mathbf{T^2}$ fibers. Hence it is reasonable to expect the full $\mathbf{T^4}$ in the fiber to sit at the bottom

[4]Of course, in order to fully determine a 3-cycle we should not only specify the segment in the base, but also the two 1-cycles in the two elliptic fibrations. The 3-cycles that we call Σ_i and $\Sigma_{i'}$ (which enter e.g. in expression 4.8) have very precise 1-cycles fibered, which are discussed in detail in appendix A.

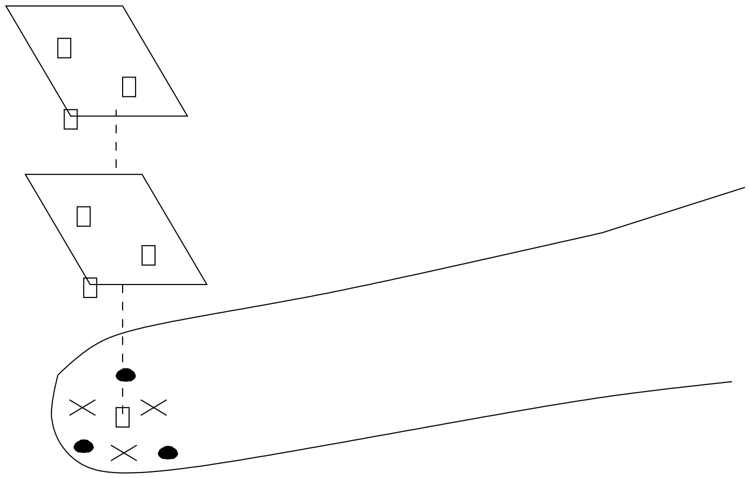

Figure 10: Structure of the throat in the z-plane, over which we have a double elliptic fibration. At its tip, round dots and crosses denote degenerations of the elliptic fibers, while square dots represent fixed points of the $\mathbb{Z}_3$ action.

of the throat. Schematically, the z-plane elongates producing the throat, all over which we have a $\mathbf{T^4}$ fibration. At the bottom of the throat, the double elliptic fibration has several degenerations, giving the $\mathbb{Z}_3$ related $\mathbf{S^3}$'s. The non-compact direction of the z-plane plays the role of the radial direction in the KS-like throat, so that there is large variation of the warp factor along that direction, and the central piece of the throat is an slice of AdS_5. In contrast with the KS throat, the internal space along the throat is not $T^{1,1}$, but rather a $\mathbf{T^2} \times \mathbf{T^2}$ bundle over $\mathbf{S^1}$. A picture of the throat and the structure at its tip is given in figure 10.

We have thus succeeded in constructing a geometry and flux background leading to a highly warped throat with orbifold singularities at its bottom. The geometry is rather involved, hence we cannot provide the explicit metric and flux density profile. We however expect that, given the analogy, its structure is similar to the KS solution. Further work to quantify this would clearly be desirable.

5. Examples of realistic models

We can now start describing some of the realistic models we can build. One can greatly benefit from the analysis in [14], which gives us the model building rules based on a local analysis, and can be applied to the throat we have just constructed.

5.1 Two scenarios

As mentioned in the introduction we may consider two main scenarios[5]

1. The standard model is embedded on a stack of anti D3-branes and D7-branes. In this construction, supersymmetry is explicitly broken on the tip of the throat. There

[5] A general discussion of the different possible scales appearing in these classes of models can be found in [21].

are different versions of this scenario (as illustrated in some of the models) where the other branes on the throat are D3- and D7- and/or $\overline{\text{D3}}$-, $\overline{\text{D7}}$-branes, but their main properties are similar. The fundamental scale at the location of these standard model branes should then be of the order of 1 TeV. This can be easily achieved from the strong redshift factor at the bottom of the throat, as in the Randall-Sundrum case. In this construction, most of the phenomenological analysis carried out for Randall-Sundrum models applies [22]. This scenario has the advantage that the anti D3-branes are dynamically attracted by the fluxes and naturally fall to the bottom of KS-like throats [13]. This reduces the number of moduli, but more importantly provides an explanation for the location of the standard model fields at the strongly redshifted region.

2. It is possible to construct supersymmetric models in the present setup, namely, if the standard model is constructed inside a stack of D3-branes. Both the D7- and D3-branes preserve the same supersymmetry and we have a version of the MSSM at the end of the throat. Additional D-branes at orbifold points away from the origin may be D3- or $\overline{\text{D3}}$ branes. In the first case supersymmetry is fully preserved on the throat, if the fluxes also preserve it. The background outside the throat may preserve supersymmetry as well (e.g. as in the F-theory example in [14, section 4.3]) or break supersymmetry (as in most models in [14]) by e.g. distant antibranes, non-supersymmetric fluxes in the CY away from the throat, etc. In both of these cases, supersymmetry breaking would be implemented via gravity mediation from a hidden sector, given by the distant non-supersymmetric source in the latter case, and from e.g. gaugino condensation or other non-perturbative effect in the former. The amount of warping on the throat in this case is not related to the hierarchy (which is stabilised by supersymmetry) and its choice would depend on the supersymmetry breaking mechanism.

5.2 Left-right models

5.2.1 Models with anti D3-branes

Consider a set of $\overline{\text{D3}}$-branes at the origin with

$$\gamma_{\theta,\bar{3}} = \text{diag}(\mathbb{1}_3, \alpha\mathbb{1}_2, \alpha^2\mathbb{1}_2)\,. \tag{5.1}$$

In order to cancel RR twisted tadpoles, we add D7-branes wrapped on the $\mathbf{T^4}$ fiber and passing through the $\mathbb{Z}_3$ point, with $\gamma_{\theta,7} = \mathbb{1}_3$. This cancels the RR twisted tadpole at the origin (2.13), but introduces tadpoles at the other fixed points. They can be cancelled by locating one anti-D3-brane at each, with $\gamma_{\theta,\bar{3}_i} = \mathbb{1}_1$.

This leads to a consistent model, which has a LR sector at the end of the throat. The spectrum in the sector of antibranes at the origin is essentially $\text{SU}(3) \times \text{SU}(2)_L \times \text{SU}(2)_R \times \text{U}(1)_{B-L}$. The additional $\overline{\text{D3}}$-branes give some abelian factors, which disappear as discussed below. The D7-branes in principle lead to an U(3) group, but the $U(1)$ factor is anomalous and becomes massive, while the SU(3) factor provides a (gauged) horizontal symmetry for leptons. The full spectrum is shown is table 1.

Matter fields	Q_3	Q_L	Q_R	Q_{D7}	$Q_{\overline{D3}^i}$	$B-L$
$\mathbf{\bar{3}\bar{3}}$ $\mathcal{N}=1$ Ch. Mults.						
$3(3,2,1;1)$	1	-1	0	0	0	$1/3$
$3(\bar{3},1,2;1)$	-1	0	1	0	0	$-1/3$
$3(1,2,2;1)$	0	1	-1	0	0	0
$\mathbf{\bar{3}7}$ Ch. Fermions						
$(1,2,1;\bar{3})$	0	1	0	-1	0	-1
$(1,1,2;3)$	0	0	-1	1	0	1
$\mathbf{\bar{3}7}$ Cmplx. Scalars						
$(3,1,1;\bar{3})$	1	0	0	-1	0	$-2/3$
$(\bar{3},1,1;3)$	-1	0	0	1	0	$2/3$
$\mathbf{\bar{3}_i7}$ Cmplx. Scalars						
$(1,1,1;\bar{3})$	0	0	0	-1	1_i	0
$(1,1,1;3)$	0	0	0	1	-1_i	0

Table 1: Spectrum of $\mathrm{SU}(3)\times\mathrm{SU}(2)_L\times\mathrm{SU}(2)_R$ model. We present the quantum numbers under the U(1) groups. The first three U(1)'s arise from the $\overline{\mathrm{D3}}$-brane sector at the origin. The next two come from the D7- and additional $\overline{\mathrm{D3}}$-brane sectors, and are written as a single column, distinguished with a label i.

There remains the crucial issue of U(1) anomalies. As discussed in [14], a 'diagonal' combination of the U(1) factors arising from the D3-branes at the origin is non-anomalous and remains massless. It is given by

$$Q_{B-L} = -2\left(\frac{1}{3}\,Q_3\ +\frac{1}{2}\,Q_L\ +\frac{1}{2}\,Q_R\right) \tag{5.2}$$

and provides the familiar $B-L$ quantum number for fields in the LR sector.

The remaining two U(1)'s and the U(1) from the D7-branes are anomalous (with anomaly cancelled by the Green-Schwarz mechanism in [17]), and become massive. Finally, the additional U(1) factors from the extra $\overline{\mathrm{D3}}$-branes have no charged fermions, and are automatically anomaly-free. However, they become massive as well, since they have non-zero $B\wedge F$ couplings with twisted closed string moduli (in analogy with the discussion in [23]). In the mentioned table we provide the charges under all U(1) factors, but list in the last column the charges under the only surviving factor (5.2).

Since we have anti D3's, the model is non-supersymmetric, as is manifest in the spectrum. However, supersymmetry is not essential in the phenomenology of the models, since the warped throat stabilises the hierarchy, a la Randall-Sundrum. This is the first semi-realistic model where the RS mechanism is put to work in an explicit string theory context.

Notice that the global geometry is different from the toroidal models in [14]. This has implications (which however do not affect the chiral structure of the LR model just constructed). For instance, it is not possible to turn on Wilson lines on the D7-brane to further break the SU(3) horizontal symmetry. In our geometry, the 1-cycles in the $\mathbf{T^4}$ fiber, on which the D7-branes wrap, are contractible so there is no moduli associated to a choice of Wilson lines. An alternative to break the D7-brane gauge group would be to introduce D7-brane world-volume magnetic fields, which are quantised and thus discrete; however we do not discuss this possibility in the present paper.

5.2.2 Models with D3-branes

Consider instead a set of D3-branes at the origin with

$$\gamma_{\theta,3} = \mathrm{diag}(\mathbb{1}_3, \alpha\mathbb{1}_2, \alpha^2\mathbb{1}_2)\,. \tag{5.3}$$

Again, in order to cancel RR twisted tadpoles, we add D7-branes with $\gamma_{\theta,7} = \mathrm{diag}(\alpha\mathbb{1}_3, \alpha^2\mathbb{1}_3)$, and one D3-brane at each of the other fixed points, with $\gamma_{\theta,3_i} = \mathbb{1}_1$ This leads to a consistent supersymmetric model, which has a LR sector at the end of the throat.

5.3 Standard model examples

It is also possible to construct local configurations with the standard model gauge group and 3 families of chiral fermions. The essential features of this class of models have been discussed in [14]. In order to illustrate their basic structure, let us consider the following particular example.

5.3.1 The standard model on anti D3-branes

Consider placing $\overline{\mathrm{D3}}$-branes at the origin, with the Chan-Paton embedding

$$\gamma_{\theta,\bar{3}} = \mathrm{diag}(\mathbb{1}_3, \alpha\mathbb{1}_2, \alpha^2\mathbb{1}_1)\,. \tag{5.4}$$

The twisted tadpole is cancelled at the origin by adding D7-branes, wrapping the fiber $\mathbf{T^4}$ and with a Chan-Paton embedding

$$\gamma_{\theta,7} = \mathrm{diag}(\mathbb{1}_6, \alpha\mathbb{1}_3)\,. \tag{5.5}$$

Again, these generate a twisted tadpole at the other fixed points, that we compensate by the addition of $\overline{\mathrm{D3}}$-branes with

$$\gamma_{\theta,\bar{3}_i} = \mathrm{diag}(\mathbb{1}_2, \alpha\mathbb{1}_1)\,. \tag{5.6}$$

The above configuration leads to the standard model gauge group $\mathrm{SU}(3)\times\mathrm{SU}(2)_L\times\mathrm{U}(1)_Y$ living in the world-volume of the $\overline{\mathrm{D3}}$-branes at the origin. Several of the extra U(1) factors of the anti-branes and from the D7-branes become massive as discussed above. The linear combination given by

$$Q_Y = -\left(\frac{1}{3}Q_3 + \frac{1}{2}Q_2 + Q_1\right) \tag{5.7}$$

is anomaly-free, remains massless, and exactly reproduces the SM hypercharge.

The $\mathrm{SU}(6)\otimes\mathrm{SU}(3)$ gauge group coming from the D7's represents an extra gauged symmetry. As pointed out in [14], the particular structure of this kind of models allows to potentially break that hidden gauge symmetry (by giving the appropriate vevs to scalar

Matter fields	Q_3	Q_2	Q_1	$Q_{D7;U(6)}$	$Q_{D7;U(3)}$	$Q_{D3;U(2),i}$	$Q_{D3;U(1),i}$	Y	Name
$\bar{\mathbf{3}}\mathbf{3}$ $\mathcal{N}=1$ Ch. Mults.									
$3(3,\bar{2};1,1;1)$	1	-1	0	0	0	0	0	$1/6$	Q_L
$3(1,2;1,1;1)$	0	1	-1	0	0	0	0	$1/2$	H_U
$3(\bar{3},1;1,1;1)$	-1	0	1	0	0	0	0	$-2/3$	U
$\bar{\mathbf{3}}\mathbf{7}$ Ch. Ferms.									
$(\bar{3},1;1,3;1)$	-1	0	0	0	1	0	0	$1/3$	D
$(1,1;6,1;1)$	0	0	-1	1	0	0	0	1	E
$(1,2,;\bar{6},1;1)$	0	1	0	-1	0	0	0	$-1/2$	L
$(1,1;1,\bar{3};1)$	0	0	1	0	-1	0	0	-1	$\bar{E}$
$\bar{\mathbf{3}}\mathbf{7}$ Cmplx. Scalars									
$(\bar{3},1;6,1;1)$	-1	0	0	1	0	0	0	$1/3$	
$(3,1;\bar{6},1;1)$	1	0	0	-1	0	0	0	$-1/3$	
$(1,2,;1,\bar{3};1)$	0	1	0	0	-1	0	0	$-1/2$	H_D
$(1,2,;1,3;1)$	0	-1	0	0	1	0	0	$1/2$	
$\bar{\mathbf{3}}_{\mathbf{i}}\mathbf{7}$ Ch. Ferms.									
$(1,1;1,3;2_i)$	0	0	0	0	1	-1_i	0	0	
$(1,1;\bar{6},1;1)$	0	0	0	-1	0	0	1_i	0	
$\bar{\mathbf{3}}_{\mathbf{i}}\mathbf{7}$ Cmplx. Scalars									
$(1,1;6,1;2_i)$	0	0	0	1	0	-1_i	0	0	
$(1,1;\bar{6},1;2_i)$	0	0	0	-1	0	1_i	0	0	
$(1,1;1,\bar{3};1)$	0	0	0	0	-1	0	1_i	0	
$(1,1;1,3;1)$	0	0	0	0	1	0	-1_i	0	
$\mathbf{77}$ $\mathcal{N}=1'$ Ch. Mult.									
$3(1,1;6,\bar{3};1)$	0	0	0	1	-1	0	0	0	

Table 2: Spectrum of the $\mathrm{SU}(3)\times\mathrm{SU}(2)\times\mathrm{U}(1)$ standard model. We present the quantum numbers under the $\mathrm{SU}(3)\times\mathrm{SU}(2)$ on $\overline{\mathrm{D3}}$-branes at the origin, the $\mathrm{SU}(6)\times\mathrm{SU}(3)$ on D7-branes, the $\mathrm{SU}(2)_i$ on $\overline{\mathrm{D3}}$-branes at the i^{th} fixed point away from the origin, and also under the U(1) factors. The first three U(1)'s arise from the $\overline{\mathrm{D3}}$-brane sector at the origin, the next two come from the D7-brane sectors, and the last two from $\overline{\mathrm{D3}}$-branes away from the origin.

fields in the 77 sector) without spoiling the good hypercharge for the matter fields. This breaking may also give a mass to some exotic matter in the 37 sector. In any case, these more detailed properties are model dependent and we skip them in our discussion.

The complete spectrum for this model is displayed in table 2 of the appendix.

Clearly, the model we have worked out is just an example. There exist several other possibilities, like cancelling twisted tadpoles with $\overline{\mathrm{D7}}$-branes or adding D3-branes instead of $\overline{\mathrm{D3}}$-branes outside the origin. In any event, since the local structure around the origin is close to the above, most models are similar and inherit the same appealing properties.

5.3.2 The standard model on D3-branes

Let us now describe a similar construction using D3-branes instead. We introduce a set of D3-branes at the origin, with

$$\gamma_{\theta,3} = \mathrm{diag}(\mathbb{1}_3, \alpha\mathbb{1}_2, \alpha^2\mathbb{1}_1)\,. \tag{5.8}$$

JHEP02(2004)031

Matter fields	Q_3	Q_2	Q_1	$Q_{D7;U(3)}$	$Q_{D7;U(6)}$	$Q_{D3;U(2),i}$	$Q_{D3;U(1),i}$	Y
33 $\mathcal{N}=1$ Ch. Mults.								
$3(3,\bar{2};1,1;1)$	1	-1	0	0	0	0	0	1/6
$3(1,2;1,1;1)$	0	1	-1	0	0	0	0	1/2
$3(\bar{3},1;1,1;1)$	-1	0	1	0	0	0	0	$-2/3$
37 + 73 $\mathcal{N}=1$ Ch. Mults.								
$(3,1;\bar{3},1;1)$	1	0	0	-1	0	0	0	$-1/3$
$(1,2;1,\bar{6};1)$	0	1	0	0	-1	0	0	$-1/2$
$(1,1;3,1;1)$	0	0	-1	1	0	0	0	1
$(\bar{3},1;1,6;1)$	-1	0	0	0	1	0	0	1/3
$\mathbf{3_i7+73_i}$ $\mathcal{N}=1$ Ch. Mults.								
$(1,1;\bar{3},1;2_i)$	0	0	0	-1	0	1_i	0	0
$(1,1;1,\bar{6};1_i)$	0	0	0	0	-1	0	1_i	0
$(1,1;1,6;\bar{2}_i)$	0	0	0	0	1	-1_i	0	0
77 $\mathcal{N}=1$ Ch. Mult.								
$3(1,1;3,\bar{6};1)$	0	0	0	1	-1	0	0	0

Table 3: Spectrum of the $\mathrm{SU}(3)\times\mathrm{SU}(2)\times\mathrm{U}(1)$ standard model. We present the quantum numbers under the $\mathrm{SU}(3)\times\mathrm{SU}(2)$ on D3-branes at the origin, the $\mathrm{SU}(3)\times\mathrm{SU}(6)$ on D7-branes, the $\mathrm{SU}(2)_i$ on D3-branes at the i^{th} fixed point away from the origin, and also under the U(1) factors. The first three U(1)'s arise from the D3-brane sector at the origin, the next two come from the D7-brane sectors, and the last two from D3-branes away from the origin.

The twisted tadpole is cancelled at the origin by adding D7-branes, with

$$\gamma_{\theta,7} = \mathrm{diag}(\alpha \mathbb{1}_3, \alpha^2 \mathbb{1}_6) \tag{5.9}$$

and D3-branes away from the origin with

$$\gamma_{\theta,3_i} = \mathrm{diag}(\mathbb{1}_2, \alpha \mathbb{1}_1)\,. \tag{5.10}$$

By arguments similar to the above one, this configuration leads to the standard model gauge group $\mathrm{SU}(3)\times\mathrm{SU}(2)_L\times\mathrm{U}(1)_Y$ living in the worldvolume of the D3-branes at the origin. Its spectrum is displayed in table 3.

5.4 Pati-Salam examples

It is also interesting to consider other model building possibilities. As an illustration, we construct a Pati-Salam model. Consider a set of anti D3-branes at the origin, with

$$\gamma_{\theta,\bar{3}} = \mathrm{diag}(\mathbb{1}_4, \alpha\mathbb{1}_2, \alpha^2\mathbb{1}_2)\,. \tag{5.11}$$

To cancel RR twisted tadpoles, we introduce D7-branes with $\gamma_{\theta,7} = \mathrm{diag}(\mathbb{1}_6)$, and anti D3-branes at other fixed points, with $\gamma_{\theta,\bar{3}_i} = \mathrm{diag}(\mathbb{1}_2)$.

The spectrum in the sector of the antibranes at the origin is essentially $\mathrm{SU}(3)\times\mathrm{SU}(2)\times\mathrm{SU}(2)\times\mathrm{U}(1)_Q$. The non-anomalous U(1) in this case corresponds to $Q=\frac{1}{4}Q_4+\frac{1}{2}Q_L+\frac{1}{2}Q_R$, and has no natural interpretation in terms of Pati-Salam grand unification. The full spectrum is in table 4.

Matter fields	Q_4	Q_L	Q_R	Q_{D7}	$Q_{\overline{D3}^i}$	Q
$\mathbf{\bar{3}\bar{3}}$ $\mathcal{N}=1$ Ch. Mults.						
$3(4,2,1;1;1)$	1	-1	0	0	0	$-1/4$
$3(\bar{4},1,2;1;1)$	-1	0	1	0	0	$1/4$
$3(1,2,2;1;1)$	0	1	-1	0	0	0
$\mathbf{\bar{3}7}$ Ch. Fermions						
$(1,2,1;\bar{6};1)$	0	1	0	-1	0	$1/2$
$(1,1,2;6;1)$	0	0	-1	1	0	$-1/2$
$\mathbf{\bar{3}7}$ Cmplx.Scalars						
$(4,1,1;\bar{6};1)$	1	0	0	-1	0	$1/4$
$(\bar{4},1,2;6;1)$	-1	0	0	1	0	$-1/4$
$\mathbf{\bar{3}_i 7}$ Cmplx.Scalars						
$(1,1,1;\bar{6};2_i)$	0	0	0	-1	1_i	0
$(1,1,1;6;2_i)$	0	0	0	1	-1_i	0

Table 4: Spectrum of $SU(4)\times SU(2)_L\times SU(2)_R$ model. We present the quantum numbers under the $SU(4)\times SU(2)\times SU(2)$ on $\overline{\text{D3}}$-branes at the origin, the SU(6) on D7-branes, and the $SU(2)_i$ on $\overline{\text{D3}}$-branes away from the origin, and the different U(1) groups. The first three U(1)'s arise from the $\overline{\text{D3}}$-brane sector at the origin. The next two come from the D7-branes and the additional $\overline{\text{D3}}$-brane sectors, with the latter written as a single column, distinguished with a label i.

6. Kähler moduli stabilisation

6.1 D-branes vs. anti D-branes

In the previous section we introduced two main scenarios, distinguished by whether the standard model is embedded on a stack of D3-branes or $\overline{\text{D3}}$-branes. In both scenarios we have several moduli, which are not stabilised by the fluxes. For instance, both contain geometric Kähler moduli, which include the overall CY volume (plus possibly others controlling the size of the elliptic fibers, whose existence depends on the global CY structure), and two blow-up moduli at each of the orbifold points of the geometry. These will be discussed in next subsection. In addition, in scenario 1, the standard model branes have three complex moduli, associated to the possibility of combining three fractional D3-branes into a dynamical regular D3-brane, and moving it off the orbifold point. This corresponds to a flat direction of the D3-brane gauge theory (breaking the gauge group to an unrealistic $U(2)\times U(1)$), which is not lifted by the flux background, since it does not generate soft terms on D3-branes.

In this sense scenario 2 is more attractive, because fluxes do stabilise the anti D3-branes at the bottom of the throat, i.e. they generate soft masses and lift the latter flat direction; therefore in this case the standard model group is stable. Notice that this is already a concrete improvement over the models in [14].

Finally, it is worth mentioning D7-brane moduli. Since only fractional D7-branes are involved in our constructions, moduli associated to D7-brane positions are projected out by the orbifold. Even if they were present, it is expected [24, 25] that they acquire flux-induced masses, even for imaginary self-dual flux backgrounds.

6.2 Kähler moduli stabilisation

Introduction of fluxes in general stabilises the dilaton and complex structure moduli, as we have discussed above. On the other hand, Kähler moduli are not stabilised, and remain unfixed (at leading order in α'). In order to achieve a fully realistic model, it is interesting to propose and device mechanisms to stabilise Kähler moduli. For simple situations, where the only Kähler modulus is the overall CY volume, it has been proposed in [7] that non-perturbative effects (like gaugino condensation in a 7-brane sector) may lead to its stabilisation. Moreover, full moduli stabilisation is interesting, since it is a requirement to achieve the construction of de Sitter vacua, which may be relevant to describe cosmologically interesting scenario.

In our models, the number of Kähler moduli is relatively large. There are two blow-up modes at each $\mathbb{C}^3/\mathbb{Z}_3$ singularity, adding up to a total of eighteen. In addition, when embedded in a compact space, there may be additional Kähler moduli associated to the size of the base and the sizes of the elliptic fibers.

In principle, it is possible to imagine that the latter are stabilised by a combination of gaugino condensates associated to D7-branes away from the throat as in references [7, 8, 26]. This is then doable but it is clearly very model dependent, and we will not discuss it any further. On the other hand, the Kähler moduli associated to blow-up modes should be stabilised by a mechanism present at the bottom of the throat. In principle, these Kähler moduli contribute to the gauge coupling of fractional branes sitting at the singularity. For instance, for D3-branes associated to the eigenvalue $e^{2\pi i\, ki/N}$ in γ_{θ^k} (denoted i^{th} fractional D-branes in what follows), the gauge kinetic function is given by

$$f(S, M_k) = \frac{1}{N}\left(S + \sum_{k=1}^{N-1} e^{2\pi i\, ki/N}\, M_k\right), \tag{6.1}$$

where M_k is the Kähler modulus in the k^{th} twisted sector. Hence, if the world-volume gauge theory develops a gaugino condensate, it may lead to the (at least partial) stabilisation of these moduli.

However, it seems that a large number of such gaugino condensates is required, and moreover the gauge groups on branes at singularities in our explicit models do not necessarily have such kind of non-perturbative effects.

There is however an alternative mechanism of stabilisation of twisted moduli, which is automatically implemented in a large class of models, including ours. For concreteness, let us centre on a set of $\overline{\text{D3}}$-branes at an orbifold singularity. Following [16], consider a complexified Kahler moduli M_k in the k^{th} twisted sector, and define the linear combinations

$$\Phi_i = \sum_k e^{2\pi iki/N} M_k \tag{6.2}$$

then there is a coupling between the 2-forms B_i which are the 4d duals of the RR piece in Φ_i, and the U(1) gauge boson on the i^{th} fractional $\overline{\text{D3}}$-brane, given by

$$\int_{\overline{\text{D3}}} B_i \wedge F_i \,. \tag{6.3}$$

These couplings play an essential role in the Green-Schwarz cancellation of mixed U(1) - non-abelian gauge anomalies [17]. Due to the $\mathcal{N}=1$ supersymmetry unbroken by the $\overline{\text{D3}}$-brane and the orbifold, there is a non-trivial Fayet-Illiopoulos term, given in terms of the scalars ξ_i, which are the NSNS piece of Φ_i

$$\int_{\overline{\text{D3}}} \xi_i D_i \,. \tag{6.4}$$

This leads to a D-term potential

$$V_D \;=\; \sum_i \left(\sum_a q_{I,a}\, \Psi_{i,a}\, \Psi^*_{i,a} \,+\, \xi_i \right)^2 \,, \tag{6.5}$$

where a runs through all the scalars $\Psi_{i,a}$, charged (with charge $q_{i,a}$) under the i^{th} U(1) gauge group.

In the absence of such scalars, the D-term potential leads to a mass term for the twisted moduli, and freezes them at zero vev (corresponding to the blown-down limit). On the other hand, if there are massless scalars with charges of sign opposite to the FI term, turning on the FI term triggers a vev for them, leading to a restabilisation of the vacuum, usually restoring supersymmetry. In this case, each contribution to the D-term potential leads to the stabilisation of a combination of the scalars $\Psi_{i,a}$ and the twisted moduli. Some combination of fields remains as an unstabilised direction.

One could think that this is our situation, since the $\bar{3}7$ sectors do contain scalars with charges of both signs under the $\overline{\text{D3}}$-brane world-volume U(1) gauge symmetries. Indeed, in the absence of 3-form fluxes, these scalars are massless and a non-zero FI term triggers a vev for them, leading to a vacuum restabilisation and restoration of supersymmetry. In the new vacuum, the fractional $\overline{\text{D3}}$-branes are diluted as (anti)instantons on the D7-branes. However, the presence of 3-form fluxes modifies the picture because in general they induce mass terms for these fields. This mass is given by the flux density at the orbifold point, and prevents these fields from acquiring a vev, at least for small FI terms, i.e. for small vevs for twisted moduli. Hence, there is a D-term plus flux-induced potential leading to a local minimum where both twisted moduli and charged scalars are stabilised. The masses they typically acquire are of order the string scale for twisted moduli, and of order the flux scale for the charged scalars.

On general grounds, to achieve full stabilisation the model should contain as many U(1) gauge fields as twisted moduli in the model, so that there are enough contributions to the D-term potential. In constructions like the SM in section 5.3 this seems to be the case, and full stabilisation is plausible. On the other hand, in the LR model in section 5.2, there are too few U(1)'s, and some additional mechanisms would be required.

Using this new ingredient one can in principle achieve models with realistic chiral gauge sectors, and stabilisation of twisted moduli. At energies below the flux scale, the only moduli that remains is the overall Kähler moduli (and possibly other untwisted moduli), so that one recovers the situation in [7]. Fixing the additional moduli via non-perturbative effects one can in principle achieve the construction of de Sitter string vacua.

7. Phenomenology aspects

Even though a full phenomenological analysis of these models is beyond the scope of this article, we will address here several phenomenological properties of these scenarios.

1. *Gauge Couplings*
   In the scenario with the standard model on antibranes, the scale at that brane is close to the TeV scale and then there is no natural way to expect gauge coupling unification as in the MSSM.[6] Hence the relative values of the gauge couplings at that scale should directly correspond to the experimental low-energy values. For a general $\mathbb{Z}_N$ orbifold with SM group $\mathrm{U}(3) \times \mathrm{U}(2) \times \mathrm{U}(1)^{N-2}$, hypercharge is given by

$$Q_Y = -\left(\frac{1}{3}Q_3 + \frac{1}{2}Q_2 + Q_1\right), \tag{7.1}$$

   hence its normalisation depends on the order of the twist N. In fact, as it was observed in [14], by normalising $\mathrm{U}(n)$ generators such that $\mathrm{Tr}T_a^2 = \frac{1}{2}$, the normalisation of the Y generator is

$$k_1 = \frac{5}{3} + 2(N-2)\,. \tag{7.2}$$

   This amounts to a dependence on N in the Weinberg angle, namely [14]:

$$\sin^2\theta_W = \frac{g_1^2}{g_1^2 + g_2^2} = \frac{1}{k_1 + 1} = \frac{3}{6N-4}\,. \tag{7.3}$$

   For the interesting case for us, $N = 3$, we find $\sin^2\theta_W = 3/14 = 0.2143$, which is already remarkably close to the experimental value (0.23113 ± 0.00015). Hence in these models quantum corrections are less important than in standard SUSY GUT's, for which $\sin^2\theta_W = 3/8 = 0.375$ at tree-level and the quantum effects are responsible for bringing it to the experimentally observed value.

   In reference [29, 30, 14] the intermediate scale scenario was emphasised, since the matter spectrum and the normalisation of hypercharge were such that in LR models unification is achieved at that scale, with an accuracy comparable to the SUSY GUT's in the MSSM. In our construction, the intermediate scale scenario is only realisable

[6] Unification in large extra dimension scenarios, not necessarily related to string theory, were discussed in the unwarped case in [27], which achieved fast unification from power-law, rather than logarithmic, running in the extra dimensions. In the warped case it was addressed in [28], where there is logarithmic running due to the warp factor. However, both discussions require gauge bosons living in the bulk, which is not the case in our models.

with the standard model embedded on D3-branes, so their spectra are quite similar. A detailed analysis of their possible gauge unification is beyond the scope of the present paper, but we expect similar conclusions for such models.

2. *Proton stability*
   Proton stability is an important issue given that the standard model scale is at the TeV. In the models presented, baryon number is provided by the U(1) subgroup of the color U(3), and remains an exact global symmetry to all orders in perturbation theory.[7] The reason for this is that, like in the heterotic string, in D-brane models, anomalous (and some non-anomalous) U(1)'s become massive from the $4D$ realisation of the Green-Schwarz mechanism. But unlike the heterotic case, the FI term may vanish and there is no need for any charged matter field to get a vev. The corresponding U(1) survives as a global symmetry (for a detailed discussion of this issue see for instance [31]). Hence, any violation of baryon number is non-perturbative, and is therefore exponentially suppressed.

3. *Yukawa couplings*
   The structure of Yukawa couplings may be discussed as in [14], if we momentarily ignore the effect of fluxes. In configurations of D3- (or anti D3)-branes at singularities, the Yukawa couplings are provided by a set of gauge invariant cubic couplings between fields in the 33 or 37 (or $\bar{3}\bar{3}$ and $\bar{3}7$) open string sectors, in two possible structures: $(33)_1 \cdot (33)_2 \cdot (33)_3$, and $(33)_3 \cdot (37) \cdot (73)$, where the subindex denotes the associated complex plane. The first structure is responsible for providing masses for the up quarks (and the down quarks as well in LR models), and as discussed in [14] leads to two degenerate and one massless quark, as in standard untwisted sectors of orbifold models [32]. For models of D3-branes, the couplings of the second form have been described in [14], and lead to down quark masses in SM models. An important drawback is that neither those LR nor SM cases allow for lepton masses, since there is no gauge invariant cubic term between the down type Higgs and the leptons. In this respect, models of $\overline{\rm D3}$-branes provide some improvement, since they lead both to down quarks masses and lepton masses, due to the different quantum numbers of fields under the additional symmetries beyond the SM group. For the SM example in table 2, the relevant SM Yukawa couplings are $Q_L \cdot H_U \cdot U$, $Q_L \cdot H_D \cdot D$ and $L \cdot E \cdot H_U^*$.

   In any event, the physical Yukawa couplings will also have a dependence on the corresponding Kähler potential, which in our models is less understood than in standard compactifications. Furthermore, in our models with anti D3-branes, the effective Yukawa couplings will have important supersymmetry breaking contributions. These could be useful in yielding a realistic pattern for the spectrum of fermion masses.

4. *Soft breaking terms*
   In the above discussion we have ignored the effect of fluxes on the world-volume gauge

[7] This continuous global symmetry includes the $\mathbb{Z}_2$ symmetry mentioned in [14], but implies stronger constraints. Thus our statements here correct the discussion in [14].

theory, which can be quite important. In principle, new couplings are generated from the interaction of the open string modes with the background flux, with a typical scale provided by the flux density at the bottom of the throat, namely the local string scale. The lowest dimension operators can be extracted by following the techniques developed recently in [33, 25], and provide scalar mass terms, gaugino masses, and scalar trilinear terms for the world-volume fields.

We should distinguish diverse situations. In models with D3-branes, the fluxes do not lead to any soft terms for 33 fields, but may provide additional couplings involving the 37 fields (e.g. the mass terms mentioned in section 6.2). The only source of soft terms breaking the local supersymmetric structure must be provided by the distant sources, like antibranes away from the throat, and hence their structure is very model dependent.

A more explicit description can be provided for models with anti D3-branes. As discussed in [25], the $\bar{3}\bar{3}$ fields acquire non-vanishing soft terms, related to the tensor structure of the flux at the location of that brane. On the other hand, the structure of flux-induced operators involving $\bar{3}7$ fields has not been yet determined. In any event, the scale of these couplings is expected to be the flux density, so it is of the order of the local fundamental scale, namely the TeV scale. These constructions hence have the potential to lead to a fully phenomenologically viable set of mass terms for fields beyond the Standard Model, but a full determination of their spectrum would require explicit expressions for the metric and flux backgrounds in our construction.

8. Discussion

We have succeeded in providing an explicit construction that allows the introduction of realistic models on warped throats. The main idea in our construction is to combine configurations of branes at singularities (a very successful setup in the realisation of realistic chiral models with three quark-lepton families), with the construction of warped throats via fluxes (a successful setup in generating exponential hierarchies, fixing the moduli, obtaining de Sitter space, etc). This combines many of the successful ideas proposed during the past few years for the brane-world scenario, including a natural hierarchy, moduli stabilisation, supersymmetry breaking, etc. We emphasise that these are the first semirealistic models realising the RS generation of the electroweak/Planck hierarchy in string theory. Our construction then inherits many of the phenomenological properties of the Randall-Sundrum scenario and of models of D-branes at singularities, and has the potential to fix all moduli and obtain de Sitter space solutions. Given these promising features, a detailed phenomenological analysis of some of these models would be welcome. Some of these properties presumably require a more explicit description of the final metric and flux background in our construction, so further theoretical work on this issue is desirable.

One remarkable feature of our models is that the construction naturally introduces a $\mathbf{T^4}$ at the bottom of the throat. This is convenient, in that it allows the introduction of D7-branes, which help in the construction of models with realistic spectrum.

JHEP02(2004)031

There are many possible avenues to continue our work. A complete phenomenological analysis of some of our models would be desirable in order to set the conditions under which some of the models could be viable, issues of soft supersymmetry breaking terms, Yukawa couplings, gauge unification are more relevant in our models given that there is little room to tune parameters after the moduli are fixed. Generic properties, such as the appearance of extra Z' bosons at relatively low energy could be interesting to investigate along the lines of [34]. Also, in the explicit construction we found that the $\mathbb{Z}_3$ singularity was natural, as a possible symmetry of elliptic fibers in section 4, and convenient, because of the phenomenological virtues of D-branes at the $\mathbb{Z}_3$ singularity. It would however be interesting to explore the possible construction of warped throats with other orbifold (or non-orbifold) singularities.

There is a second mechanism to generate chiral models from D-branes, namely the intersecting brane models. It would be interesting to explore if the realistic models constructed in that approach could be also embedded in a warped throat background. In this sense, the explicit local models models built in [20] would be quite useful. Similarly, it would be interesting to explore the possibility of generalising the construction of semirealistic chiral models of magnetised D-branes with homogeneously distributed fluxes in [5, 6], to models with localised fluxes leading to strongly warped throats.

In reference [35] a new source of hierarchy was proposed in terms of tunnelling between multiple different throats similar to the ones discussed here, having several interesting potential implications. It may be interesting to extend our models to multi-throats and realise this effect explicitly.

The Klebanov-Strassler geometry was motivated from the gauge/gravity correspondence, as the gravitational dual of a non-conformal gauge theory. The dynamically generated chiral symmetry breaking infrared scale in the gauge theory is reproduced, in the gravity side, by the capped off throat. It would be interesting to better understand our constructions in that context, and provide a holographic gauge theory description for our more complicated structure of fluxes and cycles at the bottom of the throat. Notice that unlike Klebanov-Strassler, we do not have an explicit form of the metric defining the geometries, but certain gauge theory information may be obtained from the topological features of the model.[8]

Finally, we would like to mention the possible application of our formalism to provide concrete realistic examples of the recent attempts to obtain inflation from D-brane/anti-brane interactions in warped compactifications in string theory [36]–[38].

We expect much progress in these and other applications of the present models.

[8]Notice that the holographic interpretation of warped throats has been exploited in RS phenomenology discussions. We would like to point out a misconception in the related literature: it is often stated that the presence of SM fields in the infrared region of the throat implies that SM fields are dynamically generated bound states of the dual gauge theory. This is not the case in our constructions where SM fields can be introduced consistently in a way unrelated to the structure of the throat, and hence of the dual gauge theory side. In other words, the SM fields are present in the gravity side of the correspondence, not on the gauge theory side.

Acknowledgments

We thank R. Blumenhagen, C. Burgess, P.G. Cámara, G. Honecker, L. Ibáñez and C. de la Roza for useful conversations. J.G.C. thanks M. Pérez for her patience and affection. A.M.U. thanks DAMTP, Cambridge for hospitality when this project started, and M. González for encouragement and support. J.G.C. is supported by the Ministerio de Educación, Cultura y Deporte through a FPU grant. F.Q. is partially funded by PPARC and the Royal Society Wolfson award. M.P.G.M. is supported by a postdoctoral grant of the Consejería de Educación, Cultura, Juventud y Deportes de la Comunidad Autónoma de La Rioja (Spain). Research by A.M.U. is partially supported by CICYT, Spain.

A. Homology relation

In this appendix we prove the homology relation (4.8) by using geometric arguments. We will mainly follow the work of [20] and references therein. Let us first summarise the required tools.

Remember that our geometry consists of a double elliptic fibration over a complex plane parameterised by z. Each elliptic fibration degenerates at three points related by the $\mathbb{Z}_3$ symmetry, each labelled by the (p,q) 1-cycle that collapses on it. In our case, those 1-cycles are $(2,-1)$, $(-1,2)$, $(-1,-1)$ in each fibration. In order to distinguish the two elliptic fibrations, we adopt bare and primed labels for cycles and degeneration points, and arbitrarily call first(second) elliptic fibration to the bare(primed) one.

In going around a degeneration fiber, the 1-cycles of the elliptic fibration suffer a $\mathrm{SL}(2,\mathbb{Z})$ monodromy. A way to represent it is by considering a branch-cut in the z-plane outgoing each degeneration point. As a result, whenever one crosses (counterclockwise) the branch cut associated to a (p,q) singular point of a given elliptic fibration, the (r,s) 1-cycles in the corresponding elliptic fiber suffer a monodromy and turn into:

$$(r,s) \to (R,S) = (r,s) + I_{(r,s)(p,q)}(p,q)\,, \tag{A.1}$$

where we have defined $I_{(r,s)(p,q)} \equiv rq - sp$ the intersection number of both 1-cycles in the fiber. This is depicted in figure 11a.

Even though the location of the above branch-cuts is completely unphysical, their distribution does change the (p,q) labels of the degeneration points. We fix the ambiguity by choosing our geometry as shown in figure 12a.

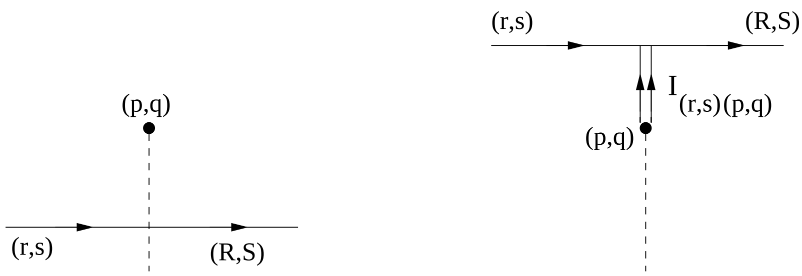

Figure 11: Prong creation process.

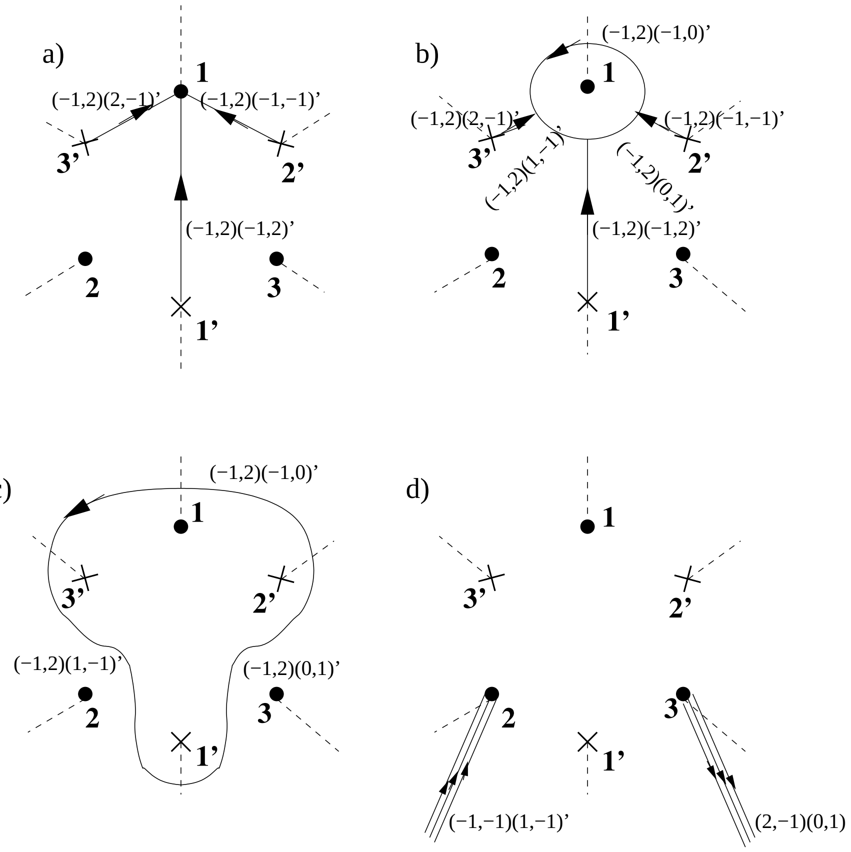

Figure 12: Deformation argument: we draw the 1-cycle in the base (z-plane) and, over each segment, specify the 2-cycle fibered over it. We describe the latter by two entries, each labelling the 1-cycle at each of the two elliptic fibrations. The notation for the singular points is $\mathbf{1}= (-1, 2)$, $\mathbf{2}= (-1,-1)$, $\mathbf{3}= (2,-1)$ (and primed), while the fibered 2-cycles are written explicitly.

An important property of the structure of degenerations in our elliptic fibration is that the 1-cycle $(1, 0)$ is invariant under the overall monodromy due to the three branch-cuts of the corresponding elliptic fiber.

Besides the compact 3-cycles considered in the main text (a segment in the base starting and ending on a degeneration point with a 2-cycle fibered over it), one may also build up "junction" compact 3-cycles. These are cycles obtained by considering networks of oriented segments in the base (for which only the external legs must end up at a degeneration point) and fibering over it the appropriate 2-cycle in the double elliptic fibration. In order to obtain a consistent 3-cycle, the fibration must be such that i) homology charge of the fibered 2-cycle is conserved at each junction and ii) segments ending on a $(p, q)/(p, q)'$ degeneration point must have the corresponding $(p, q)/(p', q')$ cycle fibered (in order for the 3-cycle to be closed).

The existence of junction 3-cycles can be derived from the prong creation process, which we will use in our computation and briefly sketch in what follows.[9] Consider a

[9]We focus on the case of just one elliptic fibration. This is the most general case for us, since we do

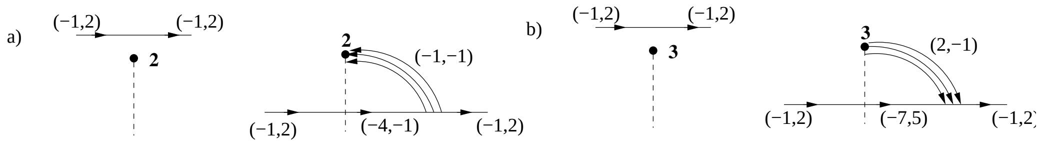

Figure 13: This is the prong creation process taking place in the last step of our deformation argument. For instance, in a), once we cross the degeneration point, the $\mathbf{1} \equiv (-1,2)$ 1-cycle in the first elliptic fibration suffers a monodromie when going through the branch-cut and becomes $(-1,2) + 3 \times (-1,-1) = (-4,-1)$. Then 3 prongs incoming the $\mathbf{2}\equiv (-1,-1)$ degeneration point emanate from the cycle and the original fibered 1-cycle $(-1,2)$ is recovered.

(r,s) cycle going through a (p,q) branch cut and thus becoming (R,S). If we move the segment across the (p,q) degeneration point, a number of prongs grow from the latter, and the original 3-cycle becomes a junction 3-cycle. The number of prongs outgoing the degeneration point is $I_{(r,s)(p,q)}$ (as required by conservation of the 2-homology charge at the junction) and necessarily have the (p,q) 1-cycle fibered over it. The process is depicted in figure 11.

We are now ready to go through the deformation argument leading to the homology relation (4.8). The different steps of the process are displayed in figure 12. For the sake of clarity in the pictures, we recall the shorthand notation already introduced in the main text, namely denote the different degeneration points by $\mathbf{1{,}2{,}3} \equiv (-1,2), (-1,-1), (2,-1)$ (and the corresponding primed labels for the second elliptic fiber).

Our starting point is the "arrow" 3-cycle of figure 12a. According to the notation introduced in section 4.5, it is representative of the homology class $-([\Pi_{11'}]+[\Pi_{12'}]+[\Pi_{13'}])$. We now grow a circle surrounding the **1** degeneration point, with the $\mathbf{1}\equiv (-1,2)$ 1-cycle over the circle, so that no prong emanates at this step. The situation looks like in figure 12*b*. Still we must choose a 1-cycle in the second elliptic fiber. Any choice would make the junction 3-cycle consistent, but we choose it to be $(-1,0)'$ so that the prongs joining it to the primed degeneration points disappear at a later stage.

We now deform the cycle in the complex z-plane, crossing the three degeneration points of the primed elliptic fiber. By construction the prongs disappear and no new prongs are created, so that we are left with the situation depicted in figure 12*c*.

The final step is to deform the 3-cycle so that it crosses the last two degeneration points of the first elliptic fiber, namely **2,3**. The procedure is detailed in figure 13*a* and 13*b*, with the outcome of 3 prongs incoming **2** and three outgoing **3**. If we finally stretch away the closed curve to the infinity of the base, we are left with the final non-compact homology 3-class $3[\Sigma_2] - 3[\Sigma_3]$, thus proving the relation (4.8).

A final remark is in order. The homology relation we have obtained is valid up to a closed 3-cycle at infinity in the z-plane. In case we work with a non-compact space (equivalently, a non-compact base manifold), we can always push that cycle away to infinity and forget about it. However, when eventually embedding our setup into a compact space, the above homological relation should be considered just up to the closed cycle.

not consider degeneration points common to both elliptic fibrations. At each collapsing point/branch cut of one of the elliptic fibrations, we can completely factorise the other.

One can use these geometric arguments to explore other homology relations among the cycles we use in the main paper. The only relevant ones for our discussion are the above, and its $\mathbb{Z}_3$ related.

References

[1] See e.g. F. Quevedo, *Phenomenological aspects of D-branes*, Trieste Lectures 2002, ICTP Lecture Notes, C. Bachas et al., editors, 2003;
G. Aldazabal, L. E. Ibáñez, F. Quevedo, A.M. Uranga, as in [14];
A.M. Uranga, *Chiral four-dimensional string compactifications with intersecting D-branes*, *Class. and Quant. Grav.* **20** (2003) S373 [hep-th/0301032];
R. Blumenhagen, V. Braun, B. Körs and D. Lüst, *The standard model on the quintic*, hep-th/0210083.

[2] A. Strominger, *Superstrings with torsion*, *Nucl. Phys.* **B 274** (1986) 253;
B. de Wit, D.J. Smit and N.D. Hari Dass, *Residual supersymmetry of compactified $D = 10$ supergravity*, *Nucl. Phys.* **B 283** (1987) 165;
J. Polchinski and A. Strominger, *New vacua for type-II string theory*, *Phys. Lett.* **B 388** (1996) 736 [hep-th/9510227];
K. Becker and M. Becker, *M-theory on eight-manifolds*, *Nucl. Phys.* **B 477** (1996) 155 [hep-th/9605053];
K. Dasgupta, G. Rajesh and S. Sethi, *M-theory, orientifolds and G-flux*, *J. High Energy Phys.* **08** (1999) 023 [hep-th/9908088];
B.R. Greene, K. Schalm and G. Shiu, *Warped compactifications in M and F theory*, *Nucl. Phys.* **B 584** (2000) 480 [hep-th/0004103];
G. Curio, A. Klemm, D. Lüst and S. Theisen, *On the vacuum structure of type-II string compactifications on Calabi-Yau spaces with H-fluxes*, *Nucl. Phys.* **B 609** (2001) 3 [hep-th/0012213];
M. Haack and J. Louis, *M-theory compactified on Calabi-Yau fourfolds with background flux*, *Phys. Lett.* **B 507** (2001) 296 [hep-th/0103068];
A.R. Frey and J. Polchinski, $N = 3$ *warped compactifications*, *Phys. Rev.* **D 65** (2002) 126009 [hep-th/0201029];
S. Kachru, M.B. Schulz and S. Trivedi, *Moduli stabilization from fluxes in a simple IIB orientifold*, *J. High Energy Phys.* **10** (2003) 007 [hep-th/0201028];
J. Louis and A. Micu, *Type II theories compactified on Calabi-Yau threefolds in the presence of background fluxes*, *Nucl. Phys.* **B 635** (2002) 395 [hep-th/0202168];
P.K. Tripathy and S.P. Trivedi, *Compactification with flux on K3 and tori*, *J. High Energy Phys.* **03** (2003) 028 [hep-th/0301139];
R. D'Auria, S. Ferrara, F. Gargiulo, M. Trigiante and S. Vaula, $N = 4$ *supergravity lagrangian for type-IIB on $T^6/\mathbb{Z}_2$ in presence of fluxes and D3-branes*, *J. High Energy Phys.* **06** (2003) 045 [hep-th/0303049];
M. Berg, M. Haack and B. Körs, *An orientifold with fluxes and branes via T-duality*, *Nucl. Phys.* **B 669** (2003) 3 [hep-th/0305183].

[3] S. Gukov, C. Vafa and E. Witten, *CFT's from Calabi-Yau four-folds*, *Nucl. Phys.* **B 584** (2000) 69 [hep-th/9906070];
see also T. Taylor and C. Vafa, *RR flux on Calabi-Yau and partial supersymmetry breaking*, *Phys. Lett.* **B 474** (2000) 130;
S. Gukov, *Solitons, superpotentials and calibrations*, *Nucl. Phys.* **B 574** (2000) 169 [hep-th/9911011];

K. Behrndt and S. Gukov, *Domain walls and superpotentials from M-theory on Calabi-Yau three-folds*, *Nucl. Phys.* **B 580** (2000) 225 [hep-th/0001082].

[4] S.B. Giddings, S. Kachru and J. Polchinski, *Hierarchies from fluxes in string compactifications*, *Phys. Rev.* **D 66** (2002) 106006 [hep-th/0105097].

[5] R. Blumenhagen, D. Lüst and T.R. Taylor, *Moduli stabilization in chiral type-IIB orientifold models with fluxes*, *Nucl. Phys.* **B 663** (2003) 319 [hep-th/0303016].

[6] J.F.G. Cascales and A.M. Uranga, *Chiral 4d $N = 1$ string vacua with D-branes and NS-NS and RR fluxes*, *J. High Energy Phys.* **05** (2003) 011 [hep-th/0303024]; *Chiral 4d string vacua with D-branes and moduli stabilization*, hep-th/0311250.

[7] S. Kachru, R. Kallosh, A. Linde and S.P. Trivedi, *de Sitter vacua in string theory*, *Phys. Rev.* **D 68** (2003) 046005 [hep-th/0301240].

[8] C. Escoda, M. Gomez-Reino and F. Quevedo, *Saltatory de Sitter string vacua*, *J. High Energy Phys.* **11** (2003) 065 [hep-th/0307160].

[9] L. Randall and R. Sundrum, *A large mass hierarchy from a small extra dimension*, *Phys. Rev. Lett.* **83** (1999) 3370 [hep-ph/9905221]; *An alternative to compactification*, *Phys. Rev. Lett.* **83** (1999) 4690 [hep-th/9906064].

[10] H. Verlinde, *Holography and compactification*, *Nucl. Phys.* **B 580** (2000) 264 [hep-th/9906182].

[11] I.R. Klebanov and M.J. Strassler, *Supergravity and a confining gauge theory: duality cascades and χSB-resolution of naked singularities*, *J. High Energy Phys.* **08** (2000) 052 [hep-th/0007191].

[12] P. Candelas and X.C. de la Ossa, *Comments on conifolds*, *Nucl. Phys.* **B 342** (1990) 246.

[13] S. Kachru, J. Pearson and H. Verlinde, *Brane/flux annihilation and the string dual of a non-supersymmetric field theory*, *J. High Energy Phys.* **06** (2002) 021 [hep-th/0112197].

[14] G. Aldazabal, L.E. Ibáñez, F. Quevedo and A.M. Uranga, *D-branes at singularities: a bottom-up approach to the string embedding of the standard model*, *J. High Energy Phys.* **08** (2000) 002 [hep-th/0005067].

[15] D. Berenstein, V. Jejjala and R.G. Leigh, *The standard model on a D-brane*, *Phys. Rev. Lett.* **88** (2002) 071602 [hep-ph/0105042];
L.F. Alday and G. Aldazabal, *In quest of 'just' the standard model on D-branes at a singularity*, *J. High Energy Phys.* **05** (2002) 022 [hep-th/0203129].

[16] M.R. Douglas and G.W. Moore, *D-branes, quivers and ale instantons*, hep-th/9603167;
M.R. Douglas, B.R. Greene and D.R. Morrison, *Orbifold resolution by D-branes*, *Nucl. Phys.* **B 506** (1997) 84 [hep-th/9704151].

[17] A. Sagnotti, *A note on the Green-Schwarz mechanism in open string theories*, *Phys. Lett.* **B 294** (1992) 196 [hep-th/9210127];
L.E. Ibáñez, R. Rabadán and A.M. Uranga, *Anomalous* U(1)*'s in type-I and type-IIB $D = 4$, $N = 1$ string vacua*, *Nucl. Phys.* **B 542** (1999) 112 [hep-th/9808139].

[18] E. Cremmer, S. Ferrara, C. Kounnas and D.V. Nanopoulos, *Naturally vanishing cosmological constant in $N = 1$ supergravity*, *Phys. Lett.* **B 133** (1983) 61;
J.R. Ellis, A.B. Lahanas, D.V. Nanopoulos and K. Tamvakis, *No-scale supersymmetric standard model*, *Phys. Lett.* **B 134** (1984) 429.

[19] C. Schoen, *On fiber products of rational elliptic surfaces with section Math. Z.* **197** (1988) 177.

[20] A.M. Uranga, *Local models for intersecting brane worlds*, *J. High Energy Phys.* **12** (2002) 058 [hep-th/0208014].

[21] O. DeWolfe and S.B. Giddings, *Scales and hierarchies in warped compactifications and brane worlds*, *Phys. Rev.* **D 67** (2003) 066008 [hep-th/0208123].

[22] For reviews see for instance: V.A. Rubakov, *Large and infinite extra dimensions: an introduction*, *Phys. Usp.* **44** (2001) 871, [hep-ph/0104152];
G. Gabadadze, *Ictp lectures on large extra dimensions*, hep-ph/0308112.

[23] L.E. Ibáñez, F. Marchesano and R. Rabadán, *Getting just the standard model at intersecting branes*, *J. High Energy Phys.* **11** (2001) 002 [hep-th/0105155].

[24] P.K. Tripathy and S.P. Trivedi, as in [2]

[25] P.G. Cámara, L.E. Ibáñez and A.M. Uranga, *Flux-induced SUSY-breaking soft terms*, hep-th/0311241.

[26] C.P. Burgess, R. Kallosh and F. Quevedo, *de Sitter string vacua from supersymmetric D-terms*, *J. High Energy Phys.* **10** (2003) 056 [hep-th/0309187].

[27] K.R. Dienes, E. Dudas and T. Gherghetta, *Extra spacetime dimensions and unification*, *Phys. Lett.* **B 436** (1998) 55 [hep-ph/9803466].

[28] A. Pomarol, *Grand unified theories without the desert*, *Phys. Rev. Lett.* **85** (2000) 4004 [hep-ph/0005293];
L. Randall and M.D. Schwartz, *Unification and the hierarchy from AdS_5*, *Phys. Rev. Lett.* **88** (2002) 081801 [hep-th/0108115].

[29] G. Aldazabal, L.E. Ibáñez and F. Quevedo, *Standard-like models with broken supersymmetry from type-I string vacua*, *J. High Energy Phys.* **01** (2000) 031 [hep-th/9909172].

[30] G. Aldazabal, L.E. Ibáñez and F. Quevedo, *A D-brane alternative to the MSSM*, *J. High Energy Phys.* **02** (2000) 015 [hep-ph/0001083].

[31] L.E. Ibáñez and F. Quevedo, *Anomalous* U(1)*'s and proton stability in brane models*, *J. High Energy Phys.* **10** (1999) 001 [hep-ph/9908305].

[32] A. Font, L.E. Ibáñez, H.P. Nilles and F. Quevedo, *Yukawa couplings in degenerate orbifolds: towards a realistic* $\mathrm{SU}(3) \times \mathrm{SU}(2) \times \mathrm{U}(1)$ *superstring*, *Phys. Lett.* **B 210** (1988) 101;
A. Font, L.E. Ibáñez, F. Quevedo and A. Sierra, *The construction of 'realistic' four-dimensional strings through orbifolds*, *Nucl. Phys.* **B 331** (1990) 421.

[33] M. Grana, *MSSM parameters from supergravity backgrounds*, *Phys. Rev.* **D 67** (2003) 066006 [hep-th/0209200].

[34] D.M. Ghilencea, L.E. Ibáñez, N. Irges and F. Quevedo, *TeV-scale Z' bosons from D-branes*, *J. High Energy Phys.* **08** (2002) 016 [hep-ph/0205083].

[35] S. Dimopoulos, S. Kachru, N. Kaloper, A.E. Lawrence and E. Silverstein, *Small numbers from tunneling between brane throats*, *Phys. Rev.* **D 64** (2001) 121702 [hep-th/0104239].

[36] For a review with many references see: F. Quevedo, *Lectures on string/brane cosmology*, *Class. and Quant. Grav.* **19** (2002) 5721 [hep-th/0210292].

[37] S. Kachru et al., *Towards inflation in string theory*, *JCAP* **10** (2003) 013 [hep-th/0308055].

[38] J.P. Hsu, R. Kallosh and S. Prokushkin, *On brane inflation with volume stabilization*, *JCAP* **12** (2003) 009 [hep-th/0311077];
A. Buchel and R. Roiban, *Inflation in warped geometries*, hep-th/0311154;
H. Firouzjahi and S.H.H. Tye, *Closer towards inflation in string theory*, hep-th/0312020.